frontiers | Frontiers in Applied Mathematics and Statistics

TYPE Original Research
PUBLISHED 04 November 2022
DOI 10.3389/fams.2022.1001392

OPEN ACCESS

EDITED BY
Ramoshweu Solomon Lebelo,
Vaal University of Technology,
South Africa

REVIEWED BY
Hira Soomro,
Universiti Teknologi Petronas, Malaysia
Xinyou Meng,
Lanzhou University of
Technology, China

*CORRESPONDENCE
Nabeela Anwar
19036109-002@uog.edu.pk

SPECIALTY SECTION
This article was submitted to Mathematical Biology, a section of the journal Frontiers in Applied Mathematics and Statistics

RECEIVED 23 July 2022
ACCEPTED 28 September 2022
PUBLISHED 04 November 2022

CITATION
Anwar N, Naz S and Shoaib M (2022) Reliable numerical treatment with Adams and BDF methods for plant virus propagation model by vector with impact of time lag and density. *Front. Appl. Math. Stat.* 8:1001392. doi: 10.3389/fams.2022.1001392

Reliable numerical treatment with Adams and BDF methods for plant virus propagation model by vector with impact of time lag and density

Nabeela Anwar[1]*, Shafaq Naz[1] and Muhammad Shoaib[2]

[1]Department of Mathematics, University of Gujrat, Gujrat, Pakistan, [2]Department of Mathematics, Commission on Science and Technology for Sustainable Development in the South University Islamabad, Attock, Pakistan

Plant disease incidence rate and impacts can be influenced by viral interactions amongst plant hosts. However, very few mathematical models aim to understand the viral dynamics within plants. In this study, we will analyze the dynamics of two models of virus transmission in plants to incorporate either a time lag or an exposed plant density into the system governed by ODEs. Plant virus propagation model by vector (PVPMV) divided the population into four classes: susceptible plants [$S(t)$], infectious plants [$I(t)$], susceptible vectors [$X(t)$], and infectious vectors [$Y(t)$]. The approximate solutions for classes $S(t)$, $I(t)$, $X(t)$, and $Y(t)$ are determined by the implementation of exhaustive scenarios with variation in the infection ratio of a susceptible plant by an infected vector, infection ratio of vectors by infected plants, plants' natural fatality rate, plants' increased fatality rate owing to illness, vectors' natural fatality rate, vector replenishment rate, and plants' proliferation rate, numerically by exploiting the knacks of the Adams method (ADM) and backward differentiation formula (BDF). Numerical results and graphical interpretations are portrayed for the analysis of the dynamical behavior of disease by means of variation in physical parameters utilized in the plant virus models.

KEYWORDS

plant virus propagation model by vector (PVPMV), Adams method (ADM), backward differentiation formula (BDF), ordinary differential equations (ODEs), virus transmission, time lag

Introduction

Plants provide food for humans and many other animals. They also provide medicines, clothing fibers, and are necessary for a healthy atmosphere. Plants, on the other hand, are susceptible to diseases, which are mostly triggered by viruses. The plant is frequently killed by these viruses. As a result, virus-related crop losses cost billions of dollars annually. Virus propagation is primarily carried out by a vector; insects which bite infectious plants become infected and subsequently infect susceptible plants. Seasonal behavior is common among insect vectors. They are most active throughout the summer and almost nearly dormant during the winter. Chemical pesticides are

often employed as a control to battle vectors. Regrettably, these chemicals are not only overpriced, but they are also harmful to humans, animal life, as well as environment. Another option is to introduce a predator species, or just boost the population of one that already exists, to predate upon the insects as well as limit the virus's transmission. The vector population can be controlled with a combination of pesticides and predators. An effective mathematical model can be exploited to study the dynamics of pathogenic plant diseases. Indeed, mathematical analysis and numerical simulations are quite valuable in comprehending the dynamics of plant disease propagation and evaluating the impact of various disease control techniques.

Several mathematical models have been established to provide a detailed exposition of how to analyze, interpret, and forecast plant pathogenic farming epidemics as a mechanism for formulating and testing crop countermeasures and control measures [1–4]. A variety of epidemiology models based upon those used mostly in animal or human epidemiology have been created to assess the population ecosystem of viral infections [5–10]. The delay differential equations can be used to define relatively different formulations of epidemic proliferation. The application of delayed differential equations in epidemiological studies extends back to Van Der Plank's pioneering work [11], when these models were first proposed to represent plant diseases. The work of Van Der Plank seemed to have a limited impact on epidemic models, owing to the model hypotheses being particularly specific to plant pathology. However, a version of the Van Der Plank model has been shown to be well-suited to characterize human/animal diseases [12]. Stella et al. investigated the dynamics of the plant epidemic model and the presence and stability of distinct model equilibria. In the absence of delay, the Routh-Hurwitz criterion is employed to assess the stability of the disease free and epidemic equilibrium. In the existence of delay, the stability of epidemic equilibrium is also studied [13]. The bifurcation modulation of a fractional mosaic virus infectious disease model of Jatropha curcas with agricultural understanding and an executing delay was examined by Liu et al. Hopf bifurcation generated by the executing delay is explored for the unconstrained system by examining the corresponding characteristic equation [5]. Basir et al. developed a mathematical model that included multiple time delays as well as a Holling type-II functioning responses. The basic reproductive number and delays in time are used to determine the presence and stability of the equilibria. The delayed system's cost-effectiveness was assessed using the optimal control theory [14]. Ray et al. proposed a mathematical model to analyze

TABLE 1 Description and default parameters setting of for non-linear PVPMV [25].

Parameters	Description	Value
N	Total density of plants	100
γ	Rate of infection of a susceptible plant by an infected vector	0.01
γ_1	Infection ratio of vectors by infected plants	0.01
υ	Plants' natural fatality rate	0.1
r	Vectors' natural fatality rate	0.2
Ω	Vector replenishment rate	10
c	Plants' increased fatality rate owing to illness	0.1
m	Plants' proliferation rate	5
δ	Time delay	2

TABLE 2 Scenarios for model A and model B of non-linear PVPMV.

	Model A	Model B
Scenario 1 for the rate of infection of a susceptible plant by an infected vector		
C-1	$\gamma = 0.001$	$\gamma = 0.001$
C-2	$\gamma = 0.004$	$\gamma = 0.004$
C-3	$\gamma = 0.006$	$\gamma = 0.006$
C-4	$\gamma = 0.007$	$\gamma = 0.007$
C-5	$\gamma = 0.009$	$\gamma = 0.009$
	Model A	**Model B**
Scenario 2 for the rate at which an infected plant infects a susceptible vector		
C-1	$\gamma_1 = 0.001$	$\gamma_1 = 0.001$
C-2	$\gamma_1 = 0.002$	$\gamma_1 = 0.002$
C-3	$\gamma_1 = 0.003$	$\gamma_1 = 0.003$
C-4	$\gamma_1 = 0.004$	$\gamma_1 = 0.004$
C-5	$\gamma_1 = 0.005$	$\gamma_1 = 0.005$
	Model A	**Model B**
Scenario 3 for disease's additional fatality rate		
C-1	$c = 0.1$	$c = 0.1$
C-2	$c = 0.2$	$c = 0.2$
C-3	$c = 0.3$	$c = 0.3$
C-4	$c = 0.4$	$c = 0.4$
C-5	$c = 0.5$	$c = 0.5$
	Model A	**Model B**
Scenario 4 for the plants' natural fatality rate		
C-1	$r = 0.1$	$r = 0.1$
C-2	$r = 0.2$	$r = 0.2$
C-3	$r = 0.3$	$r = 0.3$
C-4	$r = 0.4$	$r = 0.4$
C-5	$r = 0.6$	$r = 0.6$
	Model A	**Model B**
Scenario 5:υ plants' natural fatality rate for model A, Ω vector replenishment rate for model B		
C-1	$\upsilon = 0.1$	$\Omega = 10$
C-2	$\upsilon = 0.2$	$\Omega = 100$
C-3	$\upsilon = 0.3$	$\Omega = 110$
C-4	$\upsilon = 0.4$	$\Omega = 210$
C-5	$\upsilon = 0.5$	$\Omega = 250$

the dynamics that included the incubation period as a time delay component for the vector-borne plant epidemic. The occurrence and stability of equilibrium have been investigated based on the reproduction number. Hopf bifurcation causes stability variations in the delaying and non-delaying systems [15]. Abraha et al. studied a mathematical model that included two time delays in agricultural pest management as well as the effect of farmer awareness. They assumed that the number of healthy parasites in the particular crop is proportionate to the growth of self-aware individuals. A saturation term is used to model the effects of awareness. The basic reproductive number, as well as time delays, are used to determine the presence and stability of the equilibrium. Whenever time delays reach the optimum values, stability transitions occur due to Hopf-bifurcation. The delayed system's cost-effectiveness was analyzed using adaptive control theory [16]. Phan et al. designed a system of differential equations including delay to represent the cell-to-cell propagation of infection by cereal and barley yellow dwarf pathogens throughout the plant. The model may capture a broad range of biologically pertinent phenomena through disease-free, epidemic, bilateral mortality equilibria, and a persistent periodical orbit by including a ratio-dependent incident function and logistic proliferation of healthy cells [17]. Blyuss et al. developed and analyzed a mathematical model for controlling the mosaic disease with natural microbiological biostimulants that, in addition to promoting plant development, also protect plants from infection *via* an RNA interference mechanism. They revealed how characteristics of biostimulants affect disease dynamics, and in particular, how they determine whether the mosaic disease is eliminated or preserved at a consistent level, by measuring the resilience of the system's equilibria [18]. Alemneh et al. introduced and assessed/analyzed an eco-epidemiological model of maize streak virus infection dynamics in order to evaluate the optimal strategy for preserving maize populations from the disease. To obtain an optimum controlling strategy, they applied the Pontryagin's maximum criterion to derive the Hamiltonian, control characterization, adjoint variables and the optimization system [19]. Amelia et al. presented a mathematical model of the yellow virus's spread in red chili plants, using the logistical function to predict the increase of insects as disease vectors. By calculating the dominating eigenvalue of the next generational matrix, we may determine the value of the fundamental reproduction number namely R_0 of the model [20]. Kendig et al. investigated a mathematical model

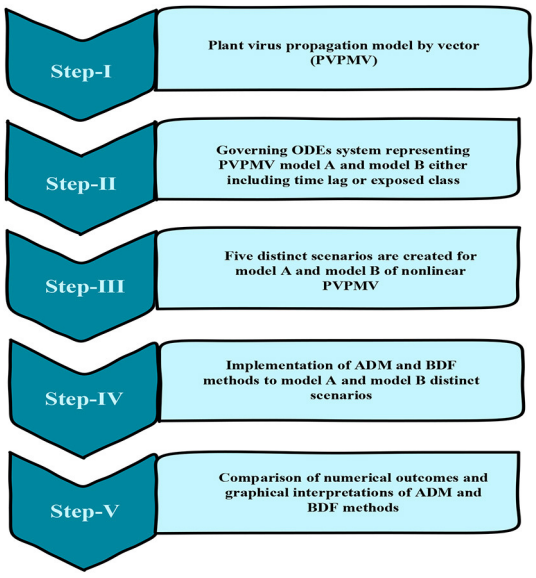

FIGURE 1
Working procedure of design approach for non-linear PVPMV.

TABLE 3 Numerical outcomes of non-linear PVPMV model A for case-1 of scenario 2.

Time (Days)	ADM Case 1				BDF Case 1			
	S	*I*	*X*	*Y*	*S*	*I*	*X*	*Y*
0	90.0000	10.0000	47.0000	47.0000	90.0000	10.0000	47.0000	47.0000
3	46.2099	53.7901	44.1326	30.5029	45.8928	54.1072	44.0134	30.1343
6	44.9054	55.0946	41.4564	22.0639	45.0189	54.9811	41.3998	21.8527
9	49.4698	50.5302	40.4576	16.9624	49.6415	50.3585	40.4446	16.8286
12	54.5650	45.4350	40.4169	13.6554	54.7283	45.2717	40.4251	13.5665
15	59.1522	40.8478	40.8143	11.4206	59.2932	40.7068	40.8314	11.3592
18	63.0405	36.9595	41.3740	9.8525	63.1582	36.8418	41.3936	9.8086
21	66.2645	33.7355	41.9611	8.7120	66.3616	33.6384	41.9803	8.6795
24	68.9206	31.0794	42.5148	7.8546	69.0006	30.9994	42.5323	7.8298
27	71.1121	28.8878	43.0115	7.1912	71.1783	28.8217	43.0270	7.1718
30	72.9859	27.0141	43.4595	6.6495	72.9307	27.0692	43.4460	6.6652

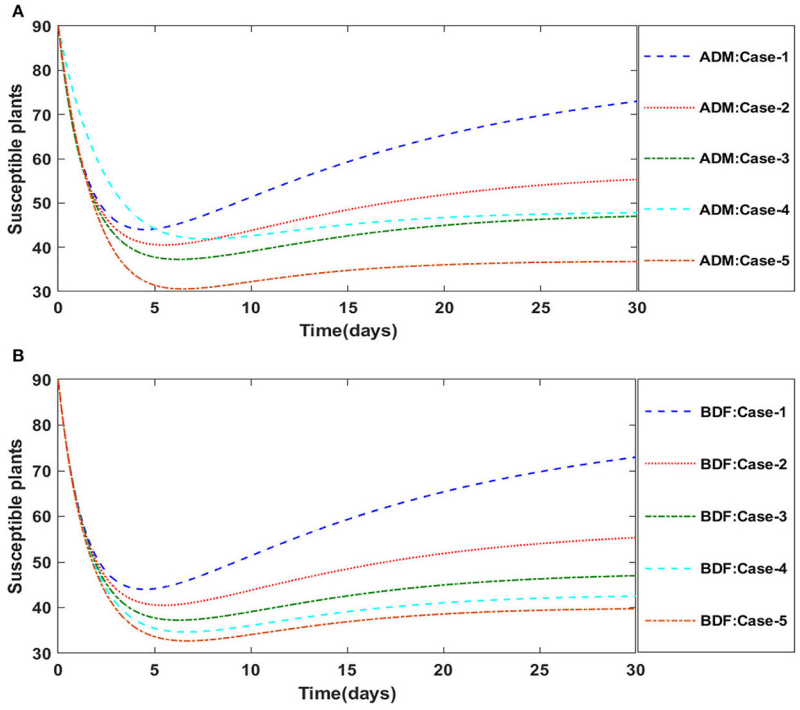

FIGURE 2
(A) Dynamics of susceptible plants for the varition in γ_1 using ADM for model A. **(B)** Dynamics of susceptible plants for the varition in γ_1 using BDF for model A.

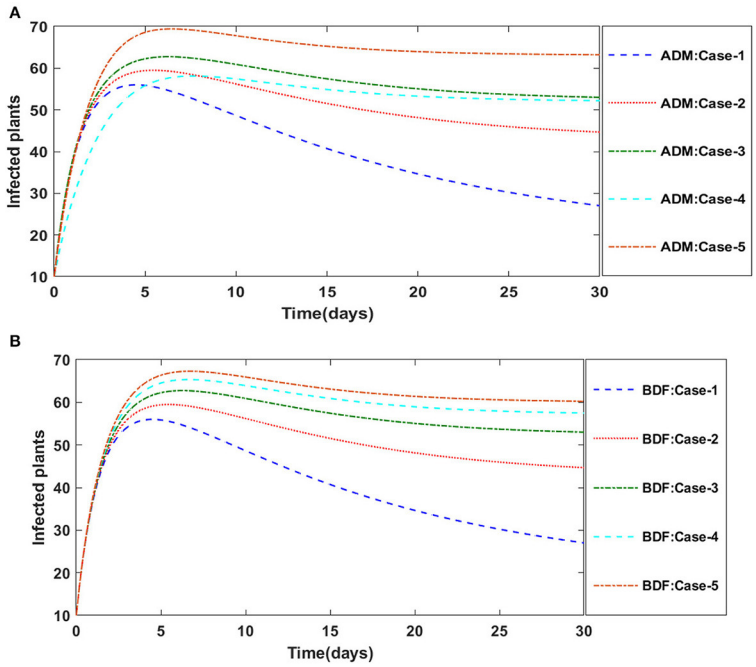

FIGURE 3
(A) Dynamics of infected plants for the varition in γ_1 using ADM for model A. **(B)** Dynamics of infected plants for the varition in γ_1 using BDF for model A.

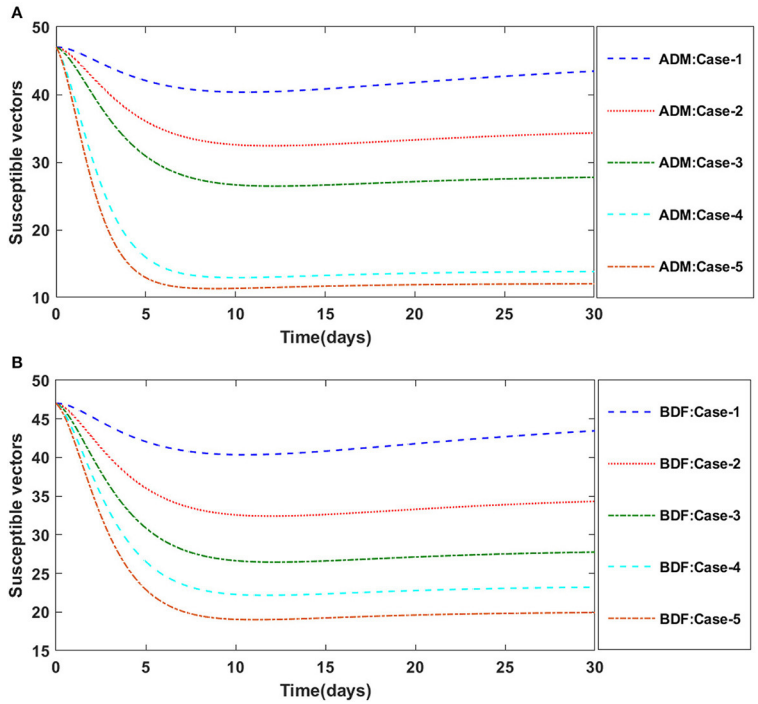

FIGURE 4
(A) Dynamics of susceptible vectors for the varition in γ_1 using ADM for model A. **(B)** Dynamics of susceptible vectors for the varition in γ_1 using BDF for model A.

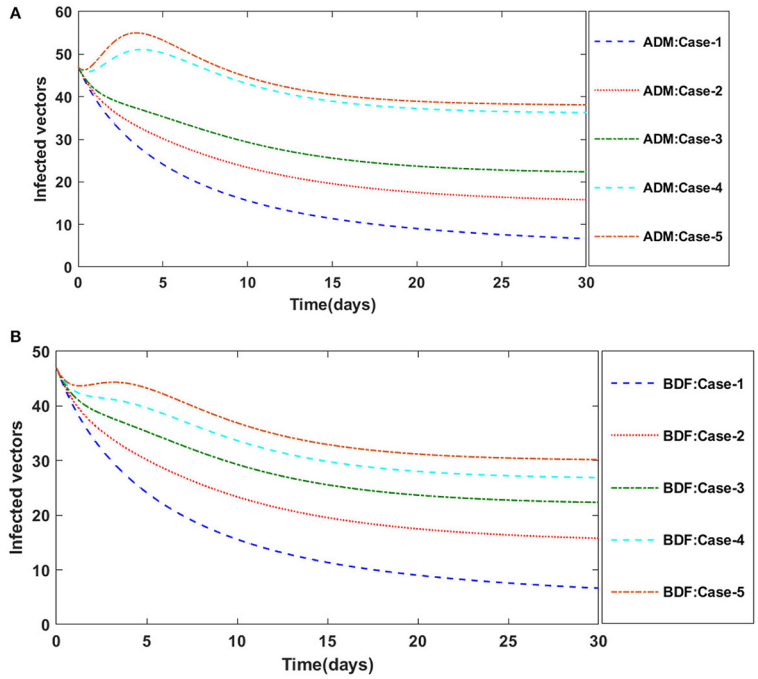

FIGURE 5
(A). Dynamics of infected vectors for the varition in γ_1 using ADM for model A. **(B)** Dynamics of infected vectors for the varition in γ_1 using BDF for model A.

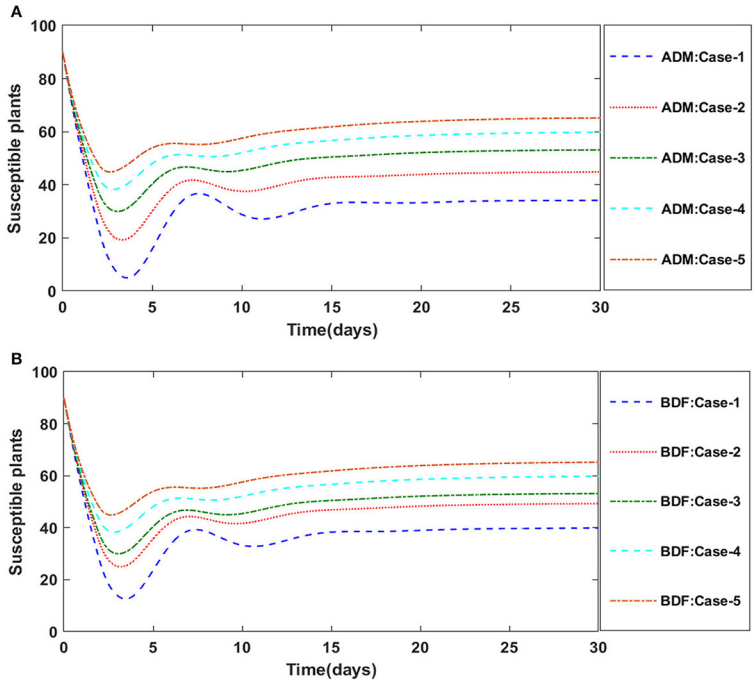

FIGURE 6
(A) Dynamics of susceptible plants for the varition in υ using ADM for model A1. **(B)** Dynamics of susceptible plants for the varition in υ using BDM for model A1.

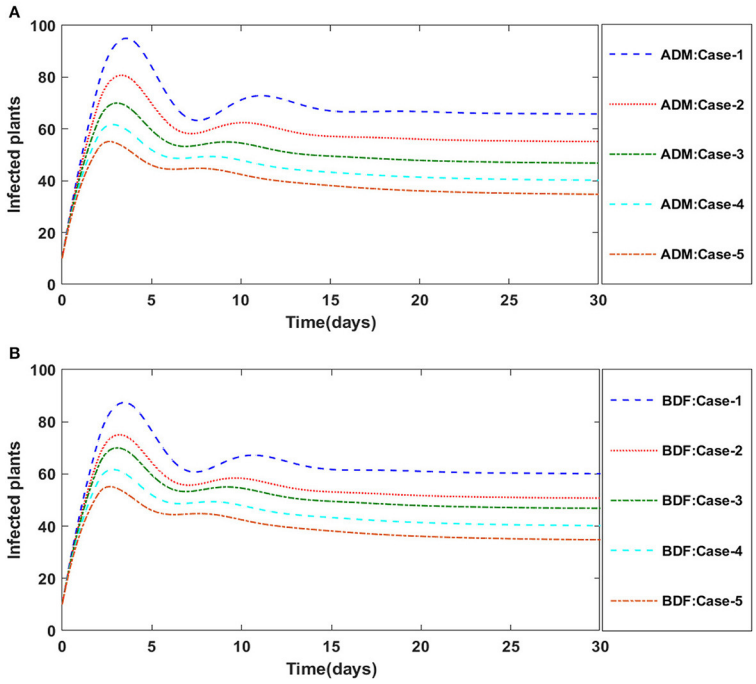

FIGURE 7
(A) Dynamics of infected plants for the varition in υ using ADM for model A1. **(B)** Dynamics of infected plants for the varition in υ using BDF for model A1.

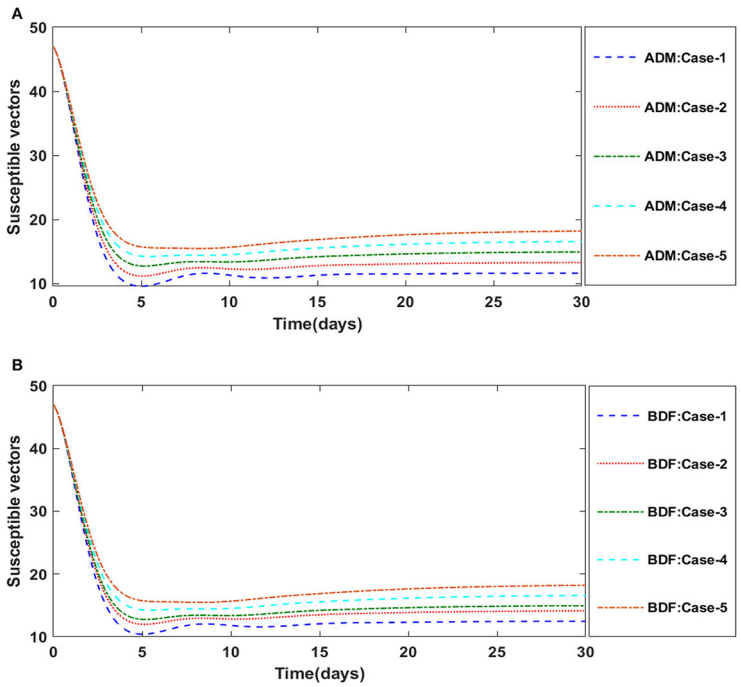

FIGURE 8
(A) Dynamics of infected plants for the varition in υ using ADM for model A1. **(B)** Dynamics of infected plants for the varition in υ using BDF for model A1.

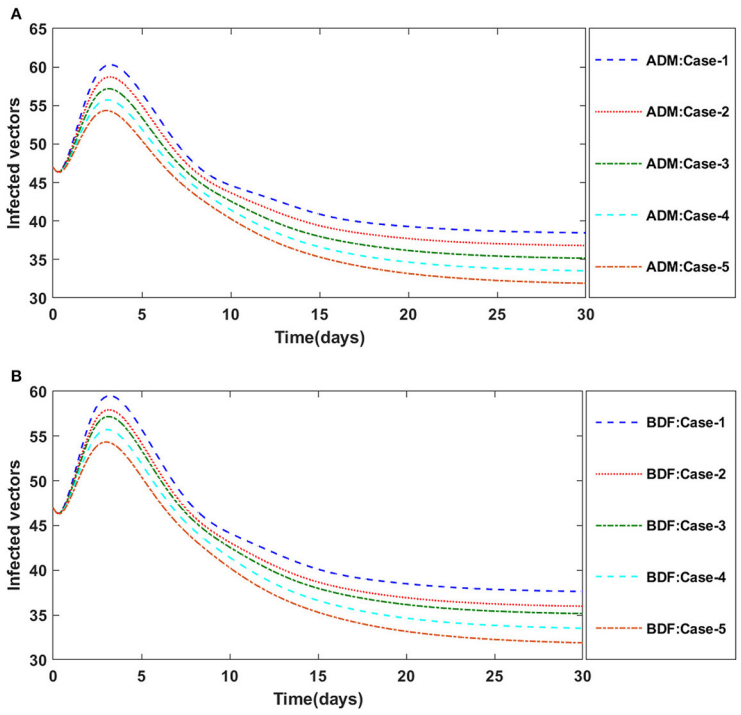

FIGURE 9
(A) Dynamics of susceptible vectors for the varition in *r* using ADM for model A1. **(B)** Dynamics of susceptible vectors for the varition in *r* using BDF for model A1.

depicting the propagation of two viruses in a plant density, parameterized assuming empirically determined transmitting values, and discovered that nutrient pathogen communication could influence disease transmission. Thus, epidemic dynamics were regulated by interactions that affected propagation through viral density-independent pathways [21]. Shaw et al. compared the model based on individual and ordinary differential equation mathematical models to investigate the impact of insect vector living cycle and behavioral factors on the transmission of vector borne plant viruses. They discovered that evacuating virus infected species proved more effective than removing vector-infested species in terms of reducing infection [22]. The interactions within the plants, vectors and predators were described by Charpentier et al. using a system of ordinary differential equations. They used direct and indirect approaches to find the controls that minimize the optimization function subjected to population factors [23]. Jittamai et al. presented a mathematical framework to analyze the dynamics for Cassava Mosaic Virus, which is accelerated by both contaminated cuttings plantings and whitefly propagation. The model was used by the authors to determine the optimal cost-effective disease control strategy [24]. Charpentier recently presented two plant virus propagation models to illustrate the two perspectives of incorporating the delays. He numerically studied the models' stability [25].

Numerical techniques are generally employed in science as well as engineering to solve mathematical problems where exact solutions are difficult or impossible to obtain. Analytical solutions are only possible for a limited differential equation. For solving ordinary differential equations, there are a variety of analytical approaches. Even though, there are many ordinary differential equations (ODEs) whose solutions can be obtained in closed form using known analytical techniques, necessitating the progression and application of numerical methods in order

TABLE 4 Numerical outcomes of non-linear PVPMV model A1 for case-1 of scenario 5.

Time (Days)	ADM Case 1				BDF Case 1			
	S	*I*	*X*	*Y*	*S*	*I*	*X*	*Y*
0	90.000	10.0000	47.0000	47.0000	90.0000	10.0000	47.0000	47.0000
3	7.253847	92.7462	13.9510	60.1967	13.8285	86.1715	14.7278	59.4199
6	28.1173	71.8826	10.0509	53.2016	33.6215	66.3785	10.7929	52.4597
9	32.5847	67.4153	11.5980	45.6751	35.5494	64.4506	12.0058	45.2673
12	27.8969	72.1031	10.8913	43.1003	34.2496	65.7504	11.5894	42.4022
15	32.9806	67.0194	11.3024	40.8883	38.2692	61.7308	12.0642	40.1265
18	33.1879	66.8121	11.5152	39.6871	38.5764	61.4236	12.2555	38.9467
21	33.4720	66.5280	11.5338	39.1260	39.1839	60.8161	12.3340	38.3258
24	33.9535	66.0464	11.6013	38.7608	39.5901	60.4099	12.4137	37.9484
27	34.0761	65.9239	11.6318	38.5669	39.7538	60.2462	12.4507	37.7480
30	34.1658	65.8342	11.6456	38.4635	39.8670	60.1330	12.4722	37.6369

TABLE 5 Numerical outcomes of non-linear PVPMV model A2 for case-1 of scenario 1.

Time (Days)	ADM Case 1				BDF Case 1			
	S	*I*	*X*	*Y*	*S*	*I*	*X*	*Y*
0	90.0000	10.0000	10.0000	47.0000	90.0000	10.0000	10.0000	47.0000
3	85.2381	17.0689	8.8230	39.7728	82.4143	20.0025	9.23605	39.4695
6	85.9571	18.0416	8.87925	36.8224	82.6595	21.6085	9.86141	36.1337
9	88.3295	16.933	8.82304	35.5548	85.0741	20.6993	10.1945	34.4088
12	90.7455	15.3976	8.47258	35.1839	87.6295	19.2833	10.0901	33.6603
15	92.7167	13.9604	7.9416	35.3571	89.7366	17.9531	9.71931	33.5382
18	94.2317	12.6973	7.3321	35.8644	91.3260	16.8256	9.24056	33.7840
21	95.2509	11.7055	6.7767	36.4903	92.4830	15.8834	8.7472	34.2194
24	96.00428	10.8327	6.2490	37.1941	93.3156	15.0854	8.28247	34.7336
27	96.5393	10.0799	5.7780	37.8979	93.9153	14.3967	7.8615	35.2635
30	96.9228	9.4206	5.36171	38.5714	94.3505	13.7927	7.4860	35.7768

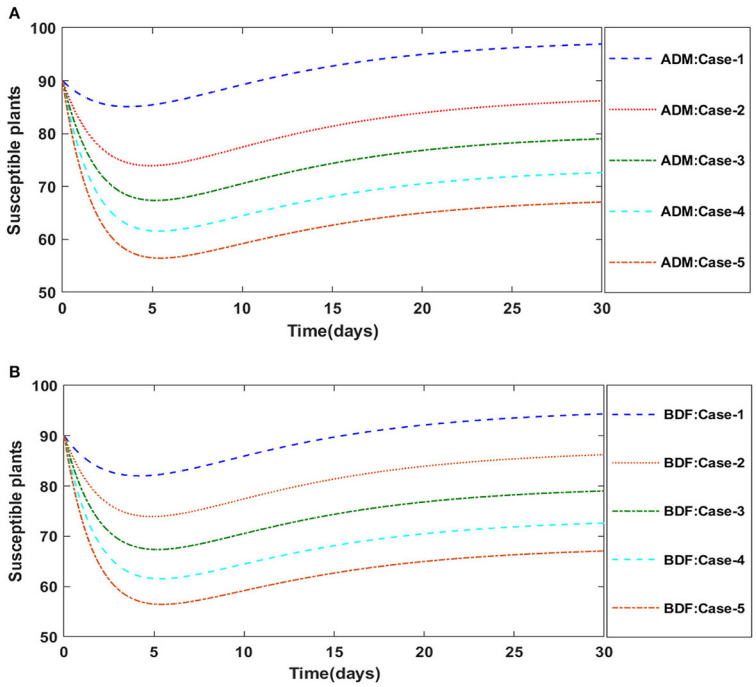

FIGURE 10
(A) Dynamics of susceptible plants for the varition in γ using ADM for model A2. **(B)** Dynamics of susceptible plants for the varition in γ using BDF for model A2.

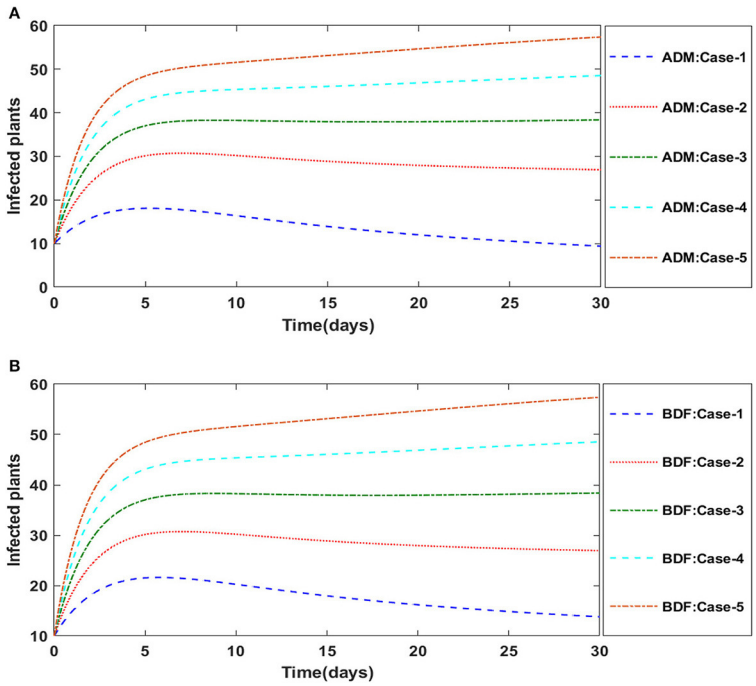

FIGURE 11
(A) Dynamics of infected plants for the varition in γ using ADM for model A2. **(B)** Dynamics of infected plants for the varition in γ using BDF for model A2.

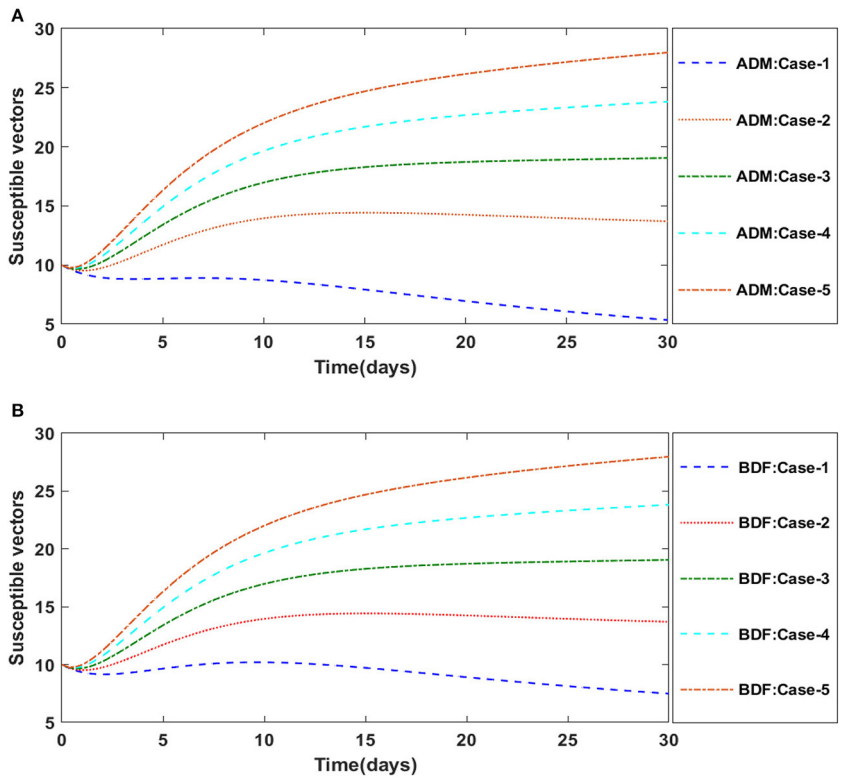

FIGURE 12
(A) Dynamics of susceptible vectors for the varition in γ using ADM for model A2. **(B)** Dynamics of susceptible vectors for the varition in γ using ADM for model A2.

to obtain the numerical solutions of a differential equation under the predefined initial condition. Various researchers have been intrigued by developing numerical techniques for solving initial value problems in ODEs in current years. Many researchers exploited various numerical techniques to approximate the solution of several mathematical models, yielding superior findings than a few of the existing ones in the literature, such as [26–30]. Recently research workers concentrated their efforts on numerically solving various mathematical models in the field of epidemiology such as COVID-19 [31], HIV model [32], tuberculosis transmission model [33], predator-prey mathematical model [34], mathematical model of cancer treatment [35]. Although the precision and stability of the aforementioned techniques are significant, they need a lot of memory and a long computation time. As a result, the numerical treatments for such approaches provide significant challenges that must be overcome in order to guarantee the precision and consistency of the solution. Therefore, ADM can be used to reliably confront one- and multi-dimensional stiff and non-stiff problems. The discrepancy between the predicted and corrected values might be used as one indicator of the error being made at each step. This gives a rather simple way to regulate the step size used in the integration. The widely used multistep ADM may approximate the solution of a first-order differential equation. In comparison to the equivalent-order Runge–Kutta method, these methods generally preserve reasonably good stability and accuracy properties while being more computationally efficient. When used with high order systems, this can significantly reduce computing time and effort. The most widely used techniques for treating stiff and non-stiff ODEs are implicit multistep techniques that utilize the BDF method. These methods were first used to confront a complex problem by Curtis and Hirschfelder [36]. Numerous implicit approaches have been created over time and are the subject of in-depth literature discussion; see [37–43]. To that end, the goal of this study is to apply the precise and stable ADM [44–48] and BDF methods to determine an initial value problem solution.

The paramount characteristics of this study are as follows: -

- The dynamics of two models of virus transmission in plants are investigated numerically to incorporate either a time lag or an exposed plant density into the system governed with non-linear delayed ODEs.
- The approximate solutions for classes $S(t)$, $I(t)$, $X(t)$, and $Y(t)$ are determined by the implementation of exhaustive

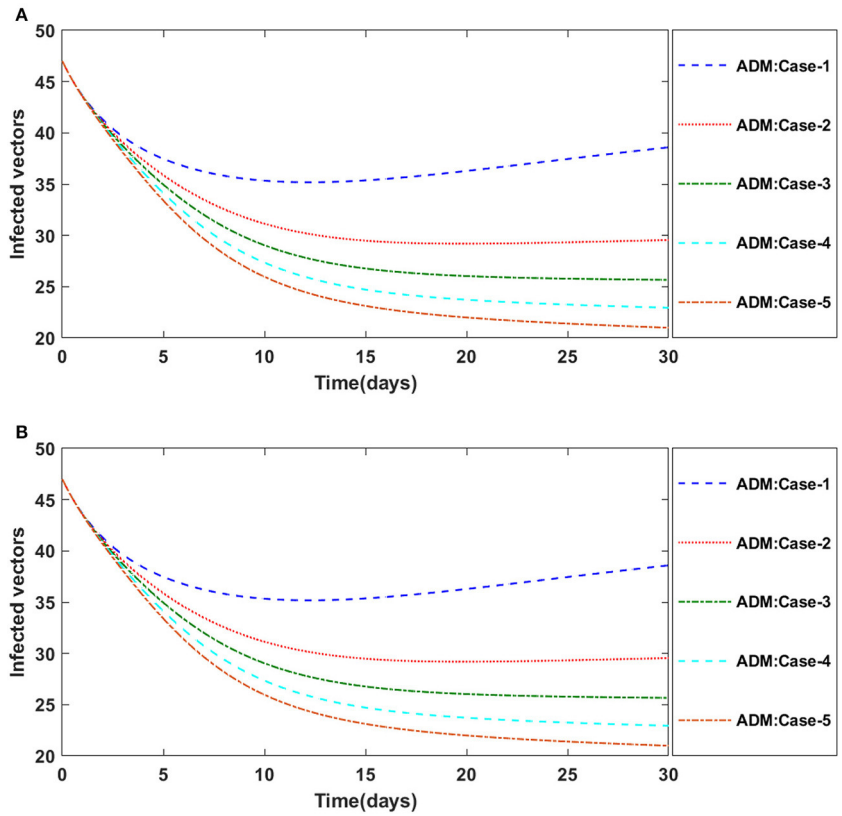

FIGURE 13
(A) Dynamics of infected vectors for the varition in γ using ADM for model A2. **(B)** Dynamics of infected vectors for the varition in γ using ADM for model A2.

TABLE 6 Numerical outcomes of nonlinear PVPMV model B for case-1 of scenario 3.

Time (Days)	ADM Case 1				BDF Case 1			
	S	*I*	*X*	*Y*	*S*	*I*	*X*	*Y*
0	30.0000	5.0000	42.0000	9.0000	30.0000	5.0000	42.0000	9.0000
3	81.2187	20.0001	34.8550	15.7049	80.6520	20.5766	34.4587	16.0901
6	64.5971	36.5518	23.2982	27.0091	64.1159	37.0125	22.9842	27.3170
9	54.1651	46.1322	16.9357	33.2329	53.9550	46.3141	16.8181	33.3472
12	50.4141	49.2806	14.8998	35.1928	87.6295	19.2833	10.0901	33.6603
15	49.4357	50.0592	14.3831	35.6677	49.4218	50.0701	14.3756	35.6742
18	49.2174	50.2283	14.2635	35.7644	49.2146	50.2304	14.2619	35.7655
21	49.1758	50.2592	14.2378	35.7775	49.1754	50.2595	14.2375	35.7775
24	49.1714	50.2617	14.2332	35.7752	49.1714	50.2616	14.2331	35.7751
27	49.1733	50.2597	14.2328	35.7718	49.1733	50.2596	14.2328	35.7717
30	49.1753	50.2578	14.2331	35.7694	49.1753	50.2577	14.2331	35.7693

scenarios with variation in the infection ratio of a susceptible plant by an infected vector, infection ratio of vectors by infected plants, plants' natural fatality rate, plants' increased fatality rate owing to illness, vectors' natural fatality rate, vector replenishment rate, and plants' proliferation rate.

- The approximate solutions of the non-linear plant virus propagation by a vector (PVPMV) are determined by

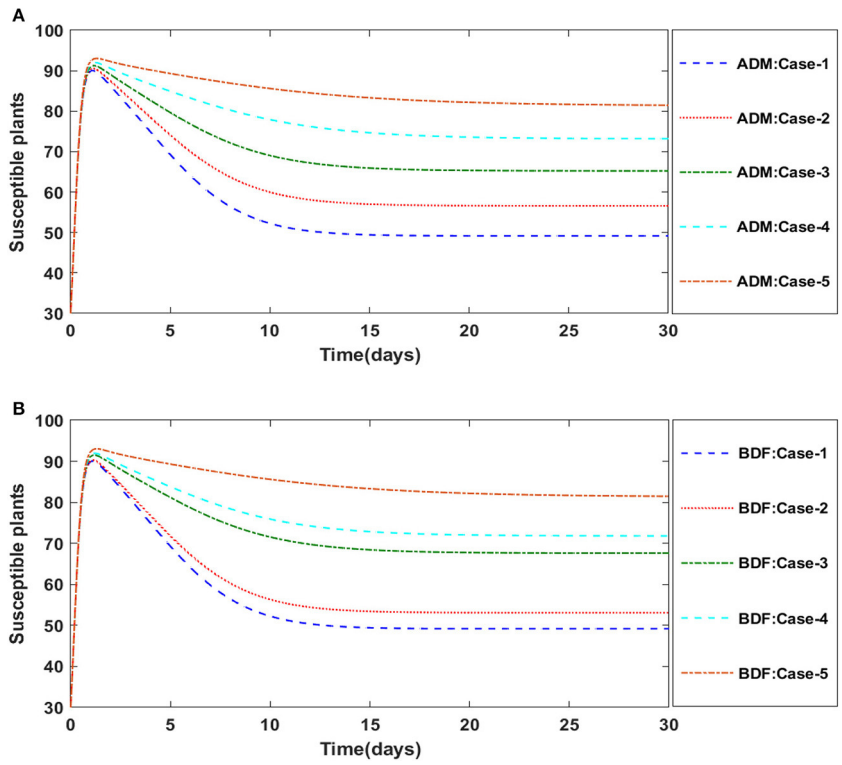

FIGURE 14
(A) Dynamics of susceptible plants for the varition in *c* using ADM for model B. **(B)** Dynamics of susceptible plants for the varition in *c* using BDF for model B.

TABLE 7 Numerical outcomes of non-linear PVPMV model B1 for case-1 of scenario 5.

Time (Days)	ADM Case 1				BDF Case 1			
	S	*I*	*X*	*Y*	*S*	*I*	*X*	*Y*
0	30.0000	5.0000	42.0000	9.0000	30.0000	5.0000	42.0000	9.0000
3	97.0808	2.6966	42.3118	8.23704	97.0728	2.70300	85.5535	10.1141
6	97.7627	2.0623	43.5322	6.7690	97.5514	2.24878	109.2329	10.9489
9	98.2168	1.6433	44.6376	5.52769	97.6434	2.15890	121.877	11.7585
12	98.5571	1.3297	45.5658	4.52489	97.5842	2.21071	128.3769	12.6420
15	98.8229	1.0848	46.3316	3.71820	97.4567	2.32606	131.4595	13.6115
18	99.0345	0.8898	46.9610	3.0663	97.2924	2.4755	132.6472	14.6478
21	99.2048	0.7329	47.4786	2.5363	97.1064	2.6450	132.7857	15.7296
24	99.3428	0.6057	47.9050	2.1033	96.9074	2.82649	132.3457	16.8395
27	99.4555	0.5019	48.2568	1.7477	96.7010	3.0148	131.5909	17.9620
30	99.5478	0.4168	48.5477	1.4548	96.4914	3.2060	130.6708	19.0838

exploiting the knacks of the Adams method (ADM) and backward differentiation formula (BDF) for sundry cases.

- Numerical and graphic interpretations of outcomes illustrate the significance/potential of these numerical methods as efficient, accurate, stable and viable computational procedures.

The remaining layout of the paper is as follows: Section Mathematical models presents mathematical models with relevant descriptions, Section Learning methodologies describes learning methodologies for the problem, Section Results and discussion provides results and discussion based on the numerical simulations,

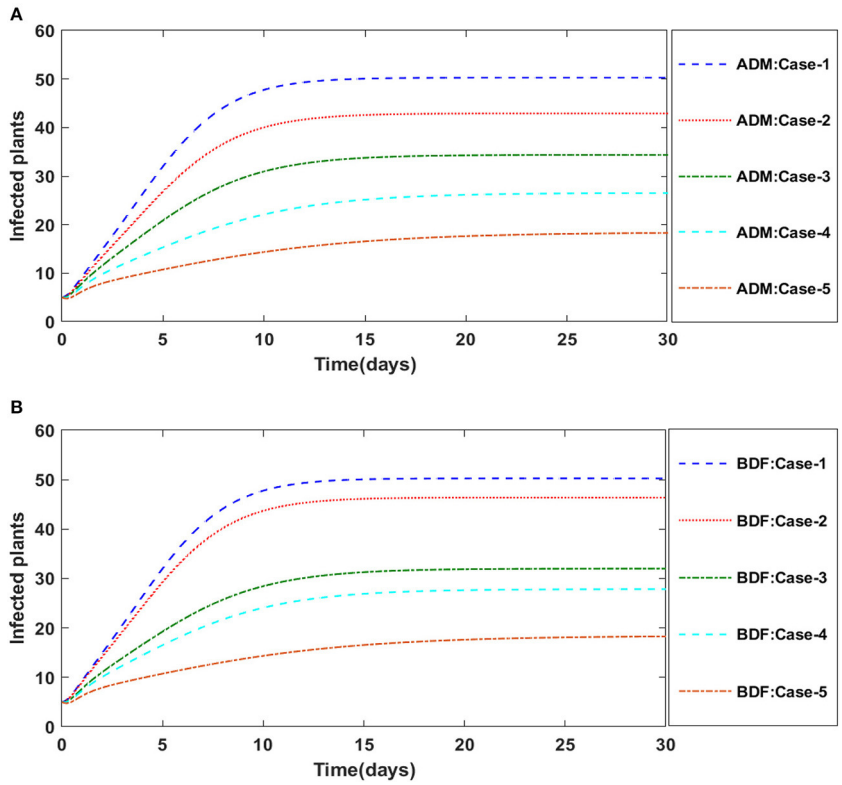

FIGURE 15
(A) Dynamics of infected plants for the varition in *d* using ADM for model B. **(B)** Dynamics of infected plants for the varition in *d* using BDF for model B.

and Section Conclusions concludes with future research recommendations.

Mathematical models

Two plant virus models are presented here in this section. The mathematical model of plant virus propagation by a vector with a constant plant density is first presented. Second, a saturated and non-constant plant density plant virus propagation model is presented.

Plant virus propagation model by a vector: Model A

We investigate two models of vector-borne plant virus transmission. Both of these are basic, and the objective is to explore how different techniques of introducing the delay affect the outcomes. There are two plant densities in the first, model A: susceptible [$S(t)$], healthier and susceptible to infection, and infectious [$I(t)$], previously infected. Because we assume that plants may not recover, we should not have a recovered class. There are also two vector populations: susceptible [$X(t)$] and infectious [$Y(t)$]. This model is a simplified form of the models provided in [49, 50].

Model A assumes that: plants as well as vectors that are new to this field, are susceptible, and the overall plant density remains stable at N because a farmer may replace any dead plants with healthy new ones, that the interaction among both the vector as well as plant is a mass movement, that the viruses decapitate plants but not the vectors who do not contract the disease, and the disease cannot be recovered from either plants or vectors. The model's parameters are the γ infection ratio of a susceptible plant by an infected vector, γ_1 infection ratio of vectors by infected plants, υ plants' natural fatality rate, c plants' increased fatality rate owing to illness, r vectors' natural fatality rate, and vector replenishment rate (according to birth or/and emigration).

Model A is represented by the system of ODEs as follows [25]:

$$S'(t) = \upsilon(N - S(t)) + cI(t) - \gamma Y(t) S(t), \quad (1)$$

$$I'(t) = \gamma Y(t) S(t) - (c + \upsilon) I(t), \quad (2)$$

$$X'(t) = \Omega - \gamma_1 I(t) X(t) - rX(t), \quad (3)$$

$$Y'(t) = \gamma_1 I(t) X(t) - rY(t). \quad (4)$$

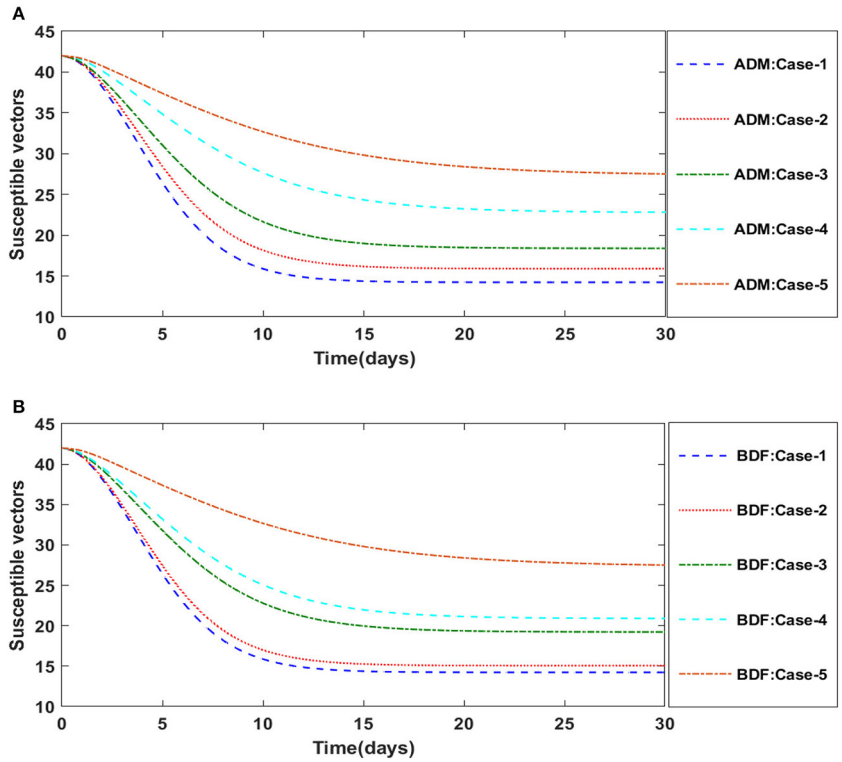

FIGURE 16
(A) Dynamics of susceptible vectors for the varition in *d* using ADM for model B. **(B)** Dynamics of susceptible vectors for the varition in *d* using BDF for model B.

There are two delays in virus transmission *via* a vector. One is being the time required for the virus to propagate throughout the plant after it has been infected. The other is the time required for the virus to propagate within the vector after it has been infected. Because the virus is not reproducing in the vector, the second is significantly smaller than the first. For the sake of simplicity, we'll assume that the second delay is zero.

We will incorporate the delays in two ways: the first is based on the premise that a susceptible needs the time delay to become infectious after coming into contact with an infectious [50, 51]. This is supposed to be model A1 [25]:

$$S'(t) = \upsilon(N - S(t)) + cI(t) - \gamma Y(t-\delta) S(t-\delta), \quad (5)$$
$$I'(t) = \gamma Y(t-\delta) S(t-\delta) - (c+\upsilon) I(t), \quad (6)$$
$$X'(t) = \Omega - \gamma_1 I(t) X(t) - rX(t), \quad (7)$$
$$Y'(t) = \gamma_1 I(t) X(t) - rY(t). \quad (8)$$

It would be possible to replace the exposed density $[E(t)]$ with a delay-accounting density. After coming into contact with an infectious, a susceptible become exposed or dormant, unable to infect. The exposed becomes infectious at the rate $\eta = 1/\delta$.

Then the model A2 will be:

$$S'(t) = \upsilon(N - S(t)) + cI(t) - \gamma Y(t) S(t) + \upsilon E(t), \quad (9)$$
$$E'(t) = \gamma Y(t) S(t) - \upsilon E(t) - \eta E(t), \quad (10)$$
$$I'(t) = \eta E(t) - (c+\upsilon) I(t), \quad (11)$$
$$X'(t) = \Omega - \gamma_1 I(t) X(t) - rX(t), \quad (12)$$
$$Y'(t) = \gamma_1 I(t) X(t) - rY(t). \quad (13)$$

Epidemic models involving an exposed class are widely known for plant virus propagation [52, 53]. Models containing exposed densities have the advantage of not requiring the initial/staring conditions to be presented at an interval equal to the delay, as delay differential equations (DDEs) require.

Plant virus propagation model by vector: Model B

We construct a further plant virus propagation model which is based on the models presented in [54, 55], but revised to include healthy vectors and mass response interactions for the disease. It takes into account four different densities:

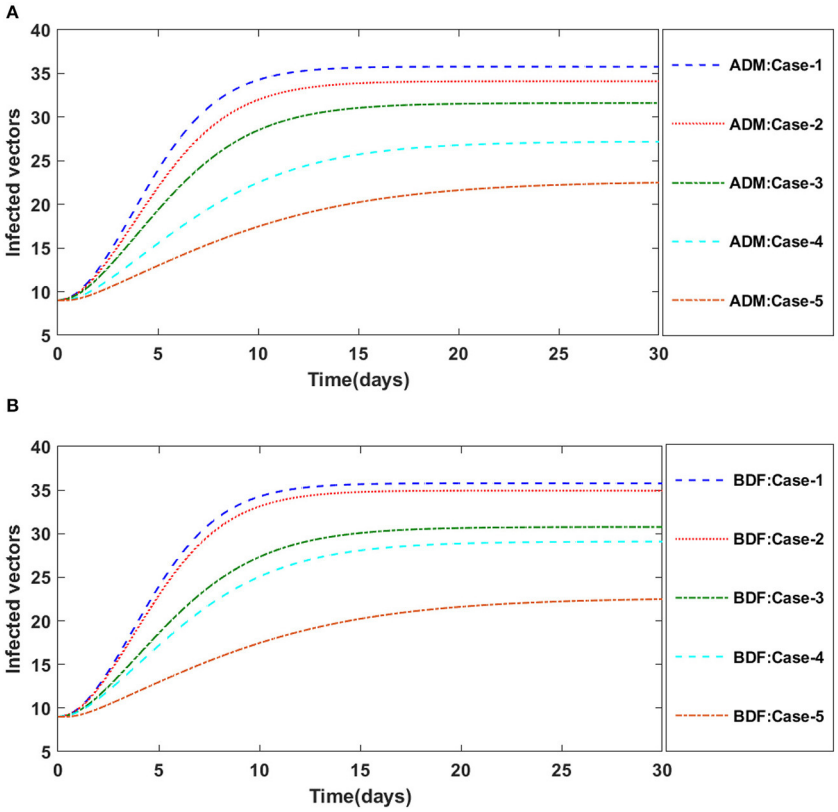

FIGURE 17
(A) Dynamics of infected vectors for the varition in *d* using ADM for model B. **(B)** Dynamics of infected vectors for the varition in *d* using BDF for model B.

susceptible plants [*S(t)*], infectious plants [*I(t)*], susceptible vectors [*X(t)*] and infectious vectors [*Y(t)*]. Because the plants grow in a logistical manner, the overall plant density does not remain constant. All emerging vectors are subject to susceptible, and their growth rate is continuously attributed to births as well as emigration. Plants are unable to recover and insects do not contract the disease, as it does in model A.

Model B, which propagates plant viruses is as follows [25]:

$$S'(t) = mS(t)\left(1 - \frac{S(t)+I(t)}{N}\right) - \frac{\gamma S(t) Y(t)}{1+\beta S(t)+aY(t)}, \quad (14)$$

$$I'(t) = \gamma S(t) Y(t) - (r+c) I(t), \quad (15)$$

$$X'(t) = \Omega - \gamma_1 I(t) X(t) - rX(t), \quad (16)$$

$$Y'(t) = \gamma_1 I(t) X(t) - rY(t). \quad (17)$$

Here, m represents the plants' proliferation rate, N their maximum capacity of carrying, and γ the rate of infection of a susceptible plant by an infected vector, r represents the plants' natural fatality rate, and c represents the virus's additional fatality rate. Ω represents the rate at which susceptible vectors are recruited, $\boldsymbol{\gamma_1}$ represents the rate at which an infected plant infects a susceptible vector, and r represents the vectors' natural fatality rate.

We will incorporate the delay in two different ways, just like we did with model A. The first assumes that a susceptible takes the time delay to get infected after coming into contact with an infected [50, 51]. Then model B* may be expressed in the form [25]:

$$S'(t) = mS(t)\left(1 - \frac{S(t)+I(t)}{N}\right) - \frac{\gamma S(t-\delta) Y(t-\delta)}{1+\beta S(t-\delta)+aY(t-\delta)}, \quad (18)$$

$$I'(t) = \frac{\gamma S(t-\delta) Y(t-\delta)}{1+\beta S(t-\delta)+aY(t-\delta)} - (r+c) I(t), \quad (19)$$

$$Y'(t) = \gamma I(t) - rY(t). \quad (20)$$

In the alternative version, we uphold [54, 55] in which the plant ceases being susceptible immediately after interaction with an infected insect, but it requires a delay period to become

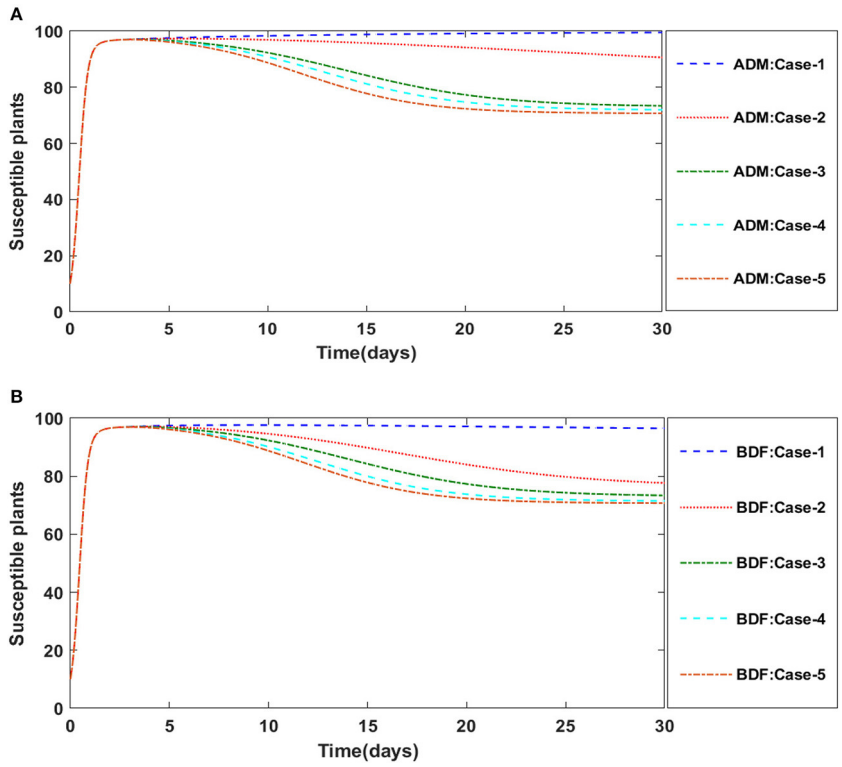

FIGURE 18
(A) Dynamics of susceptible plants for the varition in Ω using ADM for model B1. **(B)** Dynamics of susceptible plants for the varition in Ω using BDF for model B1.

infected. Because the plant could die at any time, the surviving rate is directly proportional $e^{-r\delta}$, where r is the plant's fatality rate and δ is the delay. Then model B1 will be of the form [25]:

$$\begin{aligned} S'(t) &= mS(t)\left(1-\frac{S(t)+I(t)}{N}\right) \\ &\quad -\frac{\gamma S(t)\,Y(t)}{1+\beta S(t)+aY(t)}, \qquad (21)\\ I'(t) &= e^{-r\delta}\frac{\gamma S(t-\delta)\,Y(t-\delta)}{1+\beta S(t-\delta)+aY(t-\delta)} \\ &\quad -(r+c)\,I(t), \qquad (22)\\ X'(t) &= \Omega-\gamma_1 I(t)\,X(t)-rX(t), \qquad (23)\\ Y'(t) &= \gamma_1 I(t)\,X(t)-rY(t). \qquad (24) \end{aligned}$$

A susceptible plant is infected by an infected vector at time $(t-\delta)$ in model B*, as well as the susceptible plant becomes infective at time t. A susceptible plant is infected by an infected vector that takes t to infect in model B1, with $e^{-r\delta}$ indicating the average rate of infectious susceptible who survived in time t.

Incorporating an exposed density $[E(t)]$, as before, is an alternate with the same boon and bane. The model B2 with exposed class is as follows [25]:

$$\begin{aligned} S'(t) &= mS(t)\left(1-\frac{S(t)+I(t)}{N}\right) \\ &\quad -\frac{\gamma S(t)\,Y(t)}{1+\beta S(t)+aY(t)}, \qquad (25)\\ E'(t) &= \gamma Y(t)\,S(t)-\upsilon E(t)-\eta E(t), \qquad (26)\\ I'(t) &= \eta E(t)-(c+\upsilon)\,I(t), \qquad (27)\\ X'(t) &= \Omega-\gamma_1 I(t)\,X(t)-rX(t), \qquad (28)\\ Y'(t) &= \gamma_1 I(t)\,X(t)-rY(t). \qquad (29) \end{aligned}$$

Learning methodologies

Adams method

The Adams method (ADM) is a two-step procedure for solving an ODE [56–61]. First, to use an explicit approach, the predictive step determines a crude approximation of the target number. The corrector step streamlines the preceding approximation using a different mechanism, usually an implicit one.

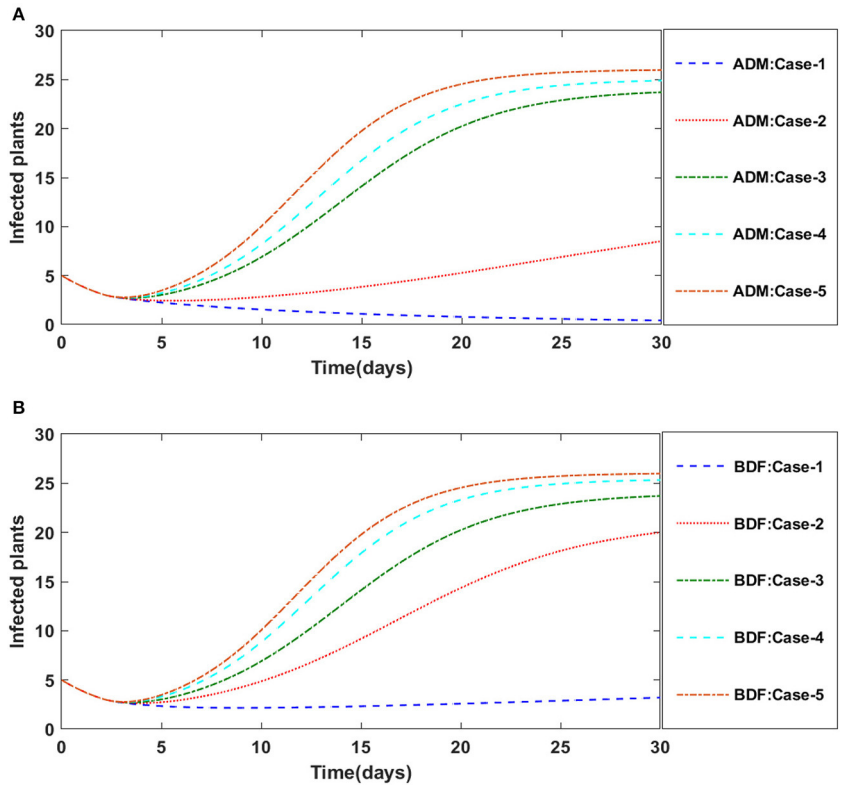

FIGURE 19
(A) Dynamics of infected plants for the varition in Ω using ADM for model B1. **(B)** Dynamics of infected plants for the varition in Ω using BDF for model B1.

The predictor-corrector technique, which is based on set of Equations (1)–(4), is represented as follows:

$$\begin{aligned}
\frac{dS}{dt} &= f\left(t, S, I, Y\right), \qquad S\left(t_0\right) = S\left(0\right), \\
\frac{dI}{dt} &= f\left(t, Y, S, I\right), \qquad I\left(t_0\right) = I\left(0\right), \\
\frac{dX}{dt} &= f\left(t, I, X\right), \qquad X\left(t_0\right) = X\left(0\right), \\
\frac{dY}{dt} &= f\left(t, I, X, Y\right), \qquad Y\left(t_0\right) = Y\left(0\right), \qquad (30)
\end{aligned}$$

To obtain a two-step predictor solution for first equation of set (30) for the non-linear plant virus propagation model by vector, use the following expression:

$$S_{k+1} = S_k + \frac{6}{4}hf\left(t_k, S_k\right) - \frac{1}{2}hf\left(t_{k-1}, S_{k-1}\right),$$

We have the following two-step corrector equation after evaluating the first equation in the nonlinear plant virus propagation model by vector:

$$S_{k+1} = S_k + \frac{1}{2}hf\left(t_{k+1}, S_{k+1}\right) + f\left(t_k, S_k\right),$$

Backward differentiation method

The backward differentiation formula (BDF) is a collection of implicit approaches for solving ordinary differential equations numerically [62–64]. They are linear multi-step algorithms that use information from previously determined time points to approximating the derivative of a function for a particular function and time, improving the precision of the approximations. These techniques are particularly useful for solving stiff differential equations [65]. In 1952, Charles F. Curtiss and Joseph O. Hirschfelder introduced the methods for the first time.

Consider the initial value problem as:

$$\frac{dz}{dt} = g\left(t, z\right), \quad z\left(t_0\right) = z_0,$$

BDF can be written in generic form as follows:

$$\sum_{m=0}^{l} c_m z_{n+m} = h\alpha g\left(t_{n+l}, z_{n+l}\right),$$

where the step size is denoted by h, g is being calculated for an unknown z_{n+l}. BDF techniques are implicit

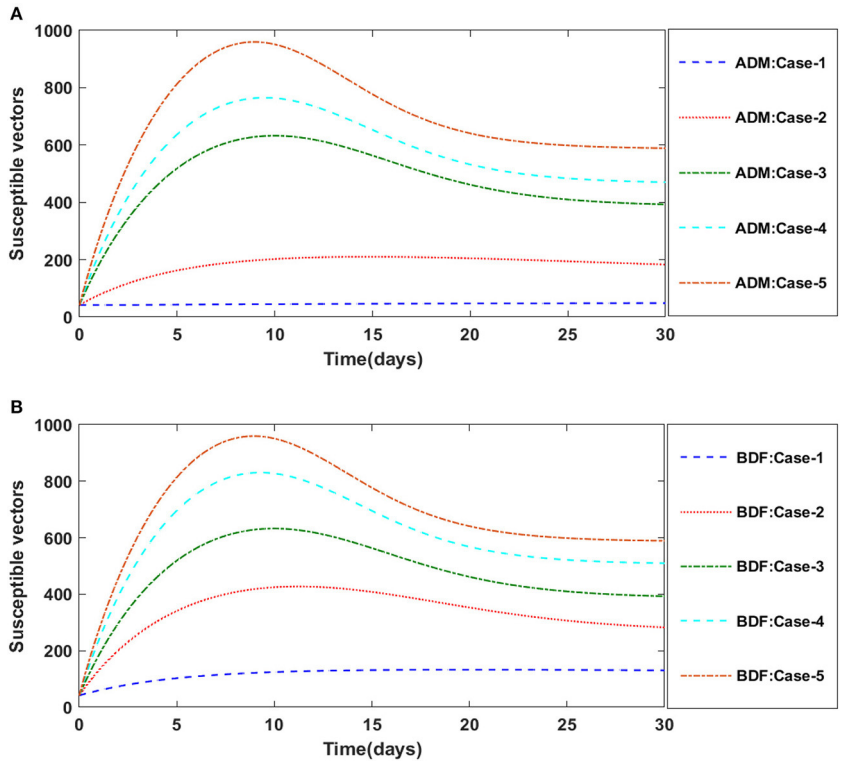

FIGURE 20
(A) Dynamics of susceptible vectors for the varition in Ω using ADM for model B1. **(B)** Dynamics of susceptible vectors for the varition in Ω using BDF for model B1.

and may require non-linear equations to be solved at each step. The coefficients c_m as well as α are considered to obtain order l, which is the highest feasible order.

Table 1 [25] lists the default settings for the non-linear PVPMV parameters, while the nomenclature describes the parameters. These default settings utilizing in all of the scenarios of non-linear PVPMV.

Results and discussion

The approximate numerical outcomes for model A [25] having a constant plant density and model B [25] having a non-constant plant density are presented in this study. The ADM and BDF methods are used to explore the dynamics of first order non-linear plant virus propagation models by a vector for three variants of models A and B, respectively with inputs from [0, 30] and step size 0.1 for cases 1–5 of each distinct scenarios of nonlinear PVPMV. As shown in Table 2, the approximate solution for the variants of model A is obtained by creating different scenarios with cases 1–5 and varying the γ infection ratio of a susceptible plant by an infected vector, γ_1 infection ratio of vectors by infected plants, υ plants' natural fatality rate, c plants' increased fatality rate owing to illness, r vectors' natural fatality rate, and Ω vector replenishment rate. Similarly, the approximate solution for the variants of model B is determined by using the impact of variation in m which represents the plants' proliferation rate, γ the rate of infection of a susceptible plant by an infected vector, r represents the plants' natural fatality rate, and c represents the disease's additional fatality rate. Ω represents the rate at which susceptible vectors are recruited, $\boldsymbol{\gamma_1}$ represents the rate at which an infected plant infects a susceptible vector, and r represents the vectors' natural fatality rate as shown in Table 2. Figure 1 depicts the working procedure of the designed approach for non-linear PVPMV.

Case study-I: Model A [25]

The three different models of plant virus propagation by a vector based on the system of ODEs without delay (model A), with delay (model A1), and without delay but including exposed class [$E(t)$] (model A2) as presented in Equations (1–4), (5–8), and (9–13) are numerically solved employing the ADM and BDF methods invoking he Mathematica routine with inputs [0, 30] and step size 0.1. Numerical outcomes and

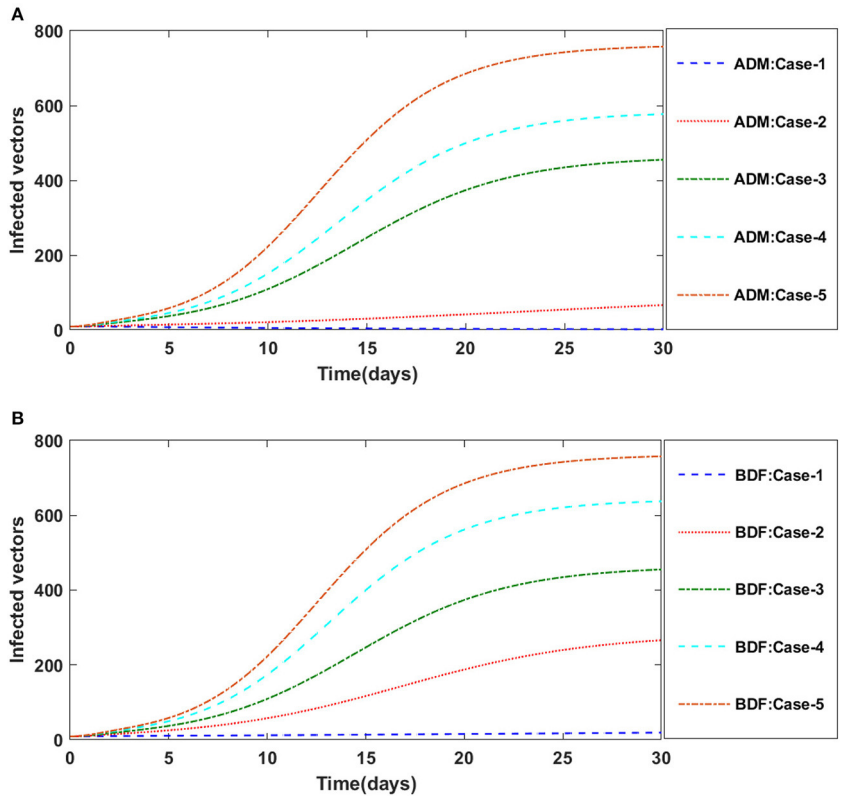

FIGURE 21
(A) Dynamics of infected vectors for the varition in Ω using ADM for model B1. **(B)** Dynamics of infected vectors for the varition in Ω using BDF for model B1.

TABLE 8 Numerical outcomes of nonlinear PVPMV model B2 for case-1 of scenario 4.

Time (Days)	ADM Case 1				BDF Case 1			
	S	*I*	*X*	*Y*	*S*	*I*	*X*	*Y*
0	30.0000	5.0000	42.0000	9.0000	30.0000	5.0000	42.0000	9.0000
3	86.3176	12.1709	12.3955	34.3073	86.6904	11.9595	12.0366	34.5894
6	73.7772	17.7705	24.1041	25.7580	74.2162	17.6038	23.6978	26.0241
9	61.1327	21.313	35.7658	19.2102	61.5174	21.2481	35.4136	19.3792
12	51.7536	21.8141	44.2058	15.5981	51.9920	21.8310	43.9967	15.6787
15	46.8476	20.9704	48.3739	14.0416	46.9494	21.0005	48.2913	14.0724
18	45.1048	20.2721	49.7273	13.5023	45.1322	20.2880	49.7077	13.5115
21	44.7574	19.9889	49.9509	13.3643	44.7596	19.9935	49.9503	13.3661
24	44.7835	19.9234	49.9091	13.3482	44.7814	19.9241	49.9111	13.3481
27	44.8401	19.9201	49.8597	13.3550	44.8386	19.9199	49.8609	13.3547
30	44.8703	19.9244	49.8356	13.3608	44.8697	19.9243	49.8361	13.3607

simulations are determined for five distinct scenarios of each model comprising cases 1–5 for non-linear PVPMV and selected random scenarios from each model for discussion. We first presented the dynamical behavior of *S(t)*, *I(t)*, *X(t)* and *Y(t)* classes of scenario 2 for model A of non-linear PVPMV. The numerical outcomes of non-linear PVPMV model A for case-1 of scenario 2 against the classes *S(t)*, *I(t)*, *X(t)* and *Y(t)* are listed in Table 3.

Figures 2A,B illustrate the dynamics of susceptible plants utilizing the ADM and BDF methods, respectively, for the

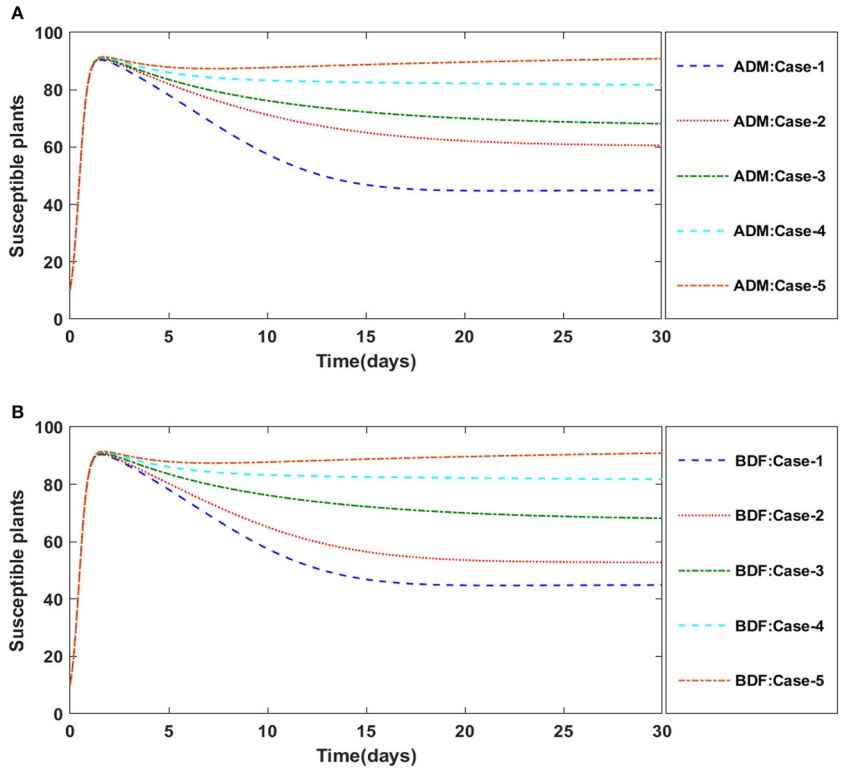

FIGURE 22
(A) Dynamics of susceptible plants for the varition in *r* using ADM for model B2. **(B)** Dynamics of susceptible plants for the varition in *r* using BDF for model B2.

variation in infection ratio of the vectors by infected plants, i.e., γ_1 for model A. It has been discovered that increasing the value of γ_1 causes the susceptible density of plants to drop. The impacts of infected plants are shown in Figures 3A,B for varied values of γ_1. As can be seen from the graph, increasing the value of γ_1 increases the density of infected plants. Figures 4A,B demonstrate that how the behavior of susceptible vectors changes as the value of γ_1 changes. For higher values of γ_1 there is an increase in the density of infected vectors. Figures 5A,B show the effects of infected vectors for various values of γ_1. Increasing the value of γ_1 increases the density of infected plants, as shown in the graphic.

The dynamics of plants' natural fatality rate i.e., υ is explored for all four classes *S(t)*, *I(t)*, *X(t)* and *Y(t)* using the strength of ADM and BDF methods for scenario 5 of the model A1. As seen in Figures 6A,B, raising the value of υ causes the density of susceptible plants to grow. The density of infected plants decreased as the value of υ increased, as seen in Figures 7A,B. Figures 8A,B show the effects of plants' natural mortality rate i.e., υ for class *X(t)* of model A1. As can be seen in the graphs, increasing the value of υ will increase the number of susceptible vectors. For class *Y(t)* of model A1, the influence of plants' natural fatality rate, i.e., υ is also computed. The rate of infected vectors reduces as the value of the infected vectors increases, as seen in Figures 9A,B. Table 4 shows the numerical outcomes of non-linear PVPMV model A1 for case-1 of scenario 5 against the classes *S(t)*, *I(t)*, *X(t)* and *Y(t)*.

Similarly, the dynamics for all four classes *S(t)*, *I(t)*, *X(t)* and *Y(t)*are analyzed by varying the infection ratio of a susceptible plant by an infected vector which is denoted by γ for scenario 1 of model A2 and graphical illustrations are presented in Figures 10–13, respectively. Numerical outcomes classes *S(t)*, *I(t)*, *X(t)* and *Y(t)* in model A2 for case-1 of scenario 1 are computed and provided in Table 5. Figures 10A,B depict the influence of the infection ratio of a susceptible plant by an infected vector on susceptible plants using the ADM and BDM methods, respectively. It is permissible to observe that when the value of γ rises, the density of susceptible plants decreases. Figures 11A,B describe the effects of the infection ratio of a susceptible plant by an infected vector on infected plants. One may observe that the density of infected plants increased in correlation with the value of γ. Figures 12A,B illustrate progressive increase in the density of susceptible vectors as the value of γ increases, whereas Figures 13A,B demonstrate the opposing behavior in the case of infected vectors.

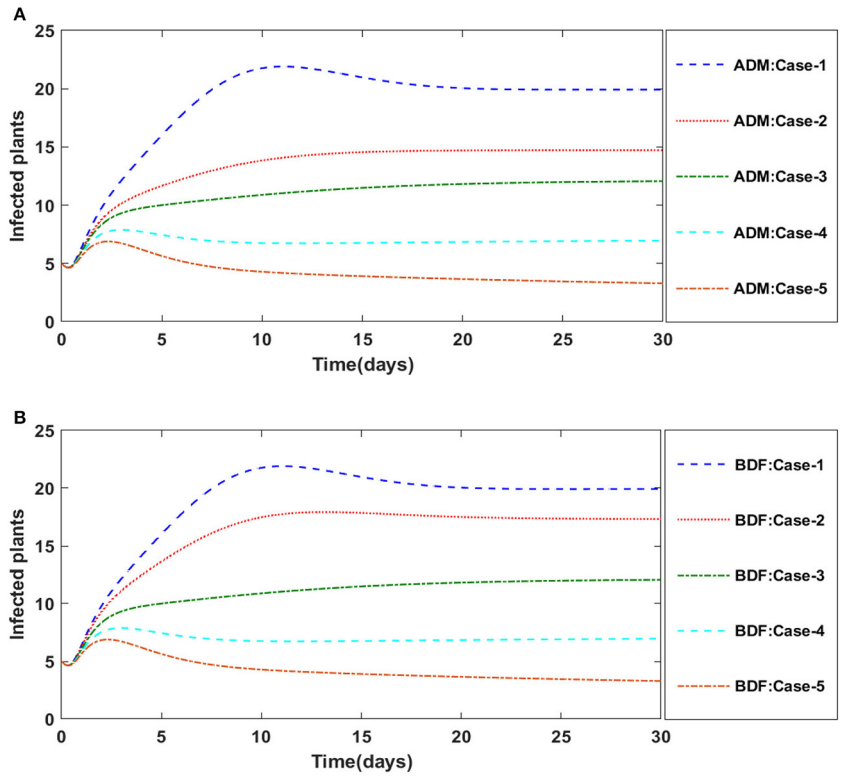

FIGURE 23
(A) Dynamics of infected plants for the varition in *r* using ADM for model B2. **(B)** Dynamics of infected plants for the varition in *r* using BDF for model B2.

Case study-II: Model B

The three segregated models of plant virus transmission by a vector, as described in Equations (14–17), (21–24), and (25–29), are numerically solved employing the ADM and BDF methods invoking the Mathematica routine. We construct five distinct scenarios incorporating cases 1–5 for non-linear PVPMV and chosen random scenarios from each model are used to determine numerical outcomes and simulations. For model B of non-linear PVPMV. We first described the dynamical behavior of the *S(t)*, *I(t)*, *X(t)*, and *Y(t)* classes in scenario 3 for the variation in disease's additional fatality rate i.e., *c*. for model B. For all four classes *S(t)*, *I(t)*, *X(t)*, and *Y(t)* numerical outcomes are determined and provided in Table 6 for case-1 of scenario 3 of model B. Figures 14A,B illustrate the dynamics of susceptible plants using the ADM and BDF methods for the variability in the disease's additional fatality rate i.e., *c*. It has been discovered that as the value of *c* is elevated, the susceptible density of plants increases. The impact of disease's additional fatality rate i.e., *c* on infected plants can be seen in Figures 15A,B. It is clear from Figures that increasing the value of *c* will result in reduction the density of infected plants. Figures 16A,B demonstrate the behavior of susceptible vectors for the variation in disease's additional fatality rate of model B. One may see that the density of susceptible vectors will increase as the value of c is increased. The influence of disease's additional fatality rate on infected vectors is presented in Figures 17A,B. It is observed from Figures that increasing the value of *c* causes the density of infected vectors to decrease.

Secondly, the dynamics of susceptible vectors' recruited rate i.e., Ω is investigated for all four classes *S(t)*, *I(t)*, *X(t)*, and *Y(t)* utilizing the strength of ADM and BDF methods for scenario 5 of the model B1 and numerical outcomes of all four classes *S(t)*, *I(t)*, *X(t)*, and *Y(t)* for the case-1 of scenario 5 is listed in Table 7. Figures 18A,B portrayed the behavior of susceptible plants density for the different values of Ω, and it is noticed that the number of susceptible plants decreases for the higher values of Ω. Figures 19A,B illustrated that as the value of Ω increases, the number of infected plants goes up. The dynmics of susceptible vectors for the variation in vectors' recruited rate i.e., *c* are presented in Figures 20A,B. One may witness that in Figures 20A,B the density of susceptible vectors goes in continous behavior for the first two cases and next three cases vectors density increased in the range of 0 to 10 days then steadily decreased and shows their steady behavior for next 20–30 days. As a result,

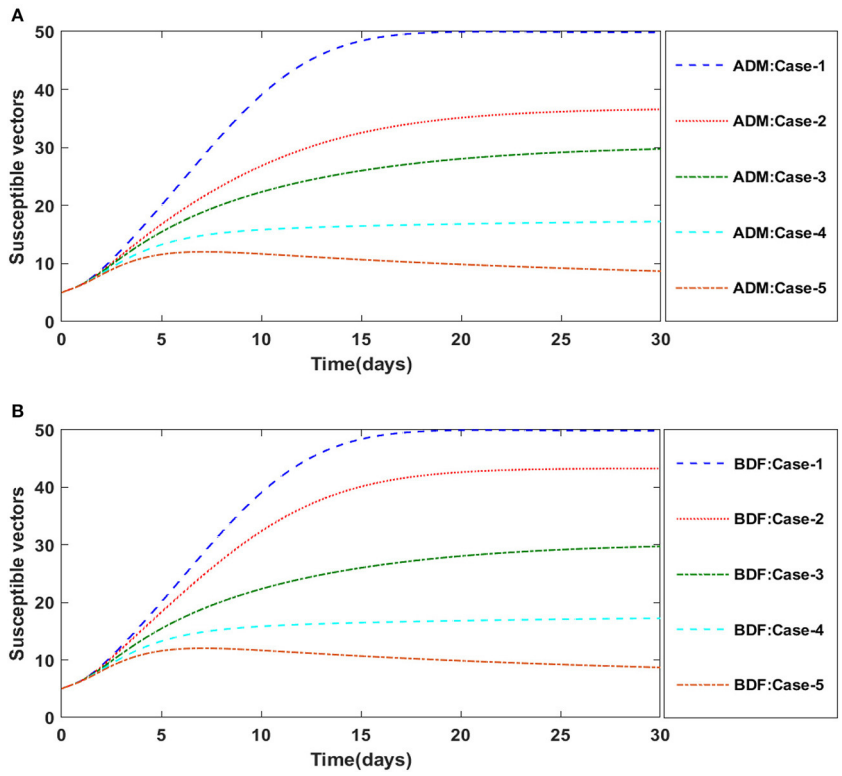

FIGURE 24
(A) Dynamics of susceptible vectors for the varition in *r* using ADM for model B2. **(B)** Dynamics of susceptible vectors for the varition in *r* using BDF for model B2.

for higher values of Ω, the density of susceptible vectors increases. Figures 21A,B portrayed the impact of susceptible vectors' recruited rate on infected vectors for model B1. The infected vectors show a steady behavior for the first two cases, also a steady behavior for the next three cases in 0–5 days, and then a gradual increase in 5–30 days, as shown in Figures 21A,B.

Finally, the dynamics of vectors' natural fatality rate i.e., *r* is investigated for all four classes *S(t)*, *I(t)*, *X(t)*, and *Y(t)* utilizing the strength of ADM and BDF methods for scenario 4 of the model B2. The respective numerical outcomes for case-1 of scenario 4 is provided in Table 8. The impact of vectors' natural fatality rate on susceptible plants is presented in Figures 22A,B As observed in graphical representation, the density of susceptible plants increased up to 90, then decreased between 3 and 10 days before returning to their steady state behavior. Also, the density of susceptible plants increased for the higher value of *r* as shown in Figures 22A,B, while the infected plants depicted reverse behavior as shown in Figures 23A,B. The influence of vectors' natural fatality rate *r* on susceptible vectors can be observed in Figures 24A,B for model B2. The number of susceptible vectors appears to decrease as the value of *r* increases. Similarly, the dynamics of infected vectors is portrayed in Figures 25A,B utilizing the ADM and BDF fro model B2, respectively. The number of infected vectors dropped as the natural fatality rate *r* of the vectors increased in model B2.

Conclusions

In this paper, we analyzed the dynamics of two models of virus transmission in plants to incorporate either a time lag or an exposed plant density into the system governed with non-linear delayed ODEs. The presented models may effectively predict susceptible plants [*S(t)*], infected plants *[I(t)*], susceptible vectors [*X(t)*], and infectious vectors [*Y(t)*]. Numerical analysis of the plant virus propagation model by a vector (PVPMV) is conducted through exhaustive scenarios with variation in different parameters used in the models. The approximate solution of the non-linear PVPMV is determined by exploiting the knacks of the Adams method (ADM) and backward differentiation formula (BDF) method We found delayed models to have a greater degree of realism since they account for the time between contact and infection. Processes are affected by delay

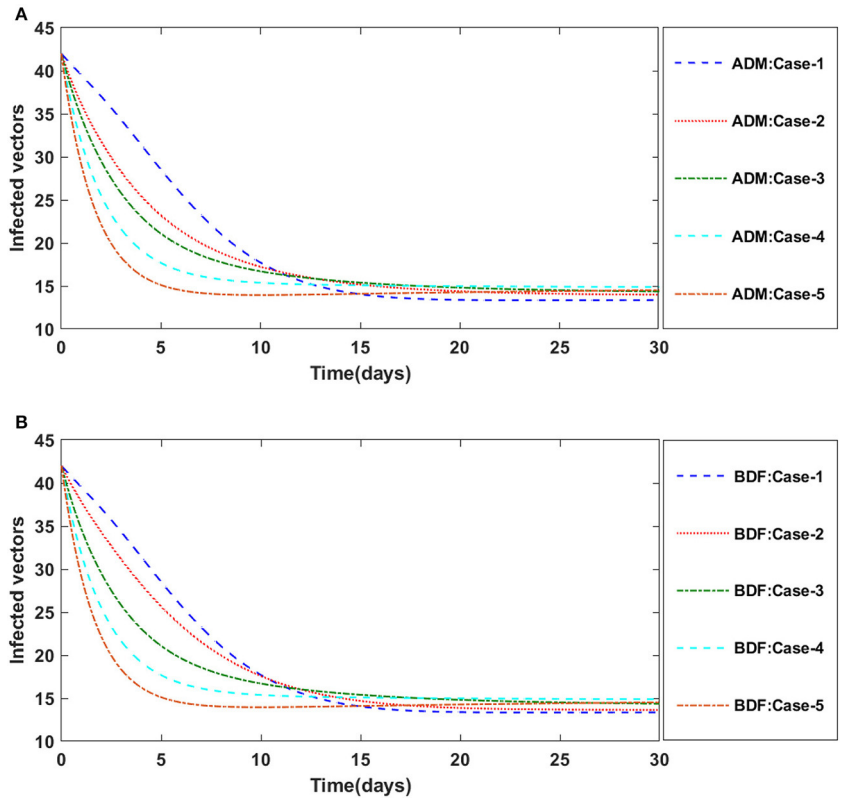

FIGURE 25
(A) Dynamics of infected vectors for the varition in *r* using ADM for model B2. **(B)** Dynamics of infected vectors for the varition in *r* using BDF for model B2.

and mathematically delay influences the dynamics along with stability. Moreover, the presented study proved to be extremely useful in controlling the plant outbreak in the subsequent seasons.

The dynamics of non-linear fluid dynamic models may be investigated in the future utilizing the strength of Adams predictor corrector method and BDF method [66–69].

Data availability statement

The original contributions presented in the study are included in the article/supplementary material, further inquiries can be directed to the corresponding author/s.

Author contributions

NA prepared methodology, results, and discussion. SN prepared introduction. MS prepared abstract and conclusion. All authors contributed to the article and approved the submitted version.

Conflict of interest

The authors declare that the research was conducted in the absence of any commercial or financial relationships that could be construed as a potential conflict of interest.

Publisher's note

All claims expressed in this article are solely those of the authors and do not necessarily represent those of their affiliated organizations, or those of the publisher, the editors and the reviewers. Any product that may be evaluated in this article, or claim that may be made by its manufacturer, is not guaranteed or endorsed by the publisher.

References

1. Rossi V, Sperandio G, Caffi T, Simonetto A, Gilioli G. Critical success factors for the adoption of decision tools in IPM. *Agronomy.* (2019) 9:710. doi: 10.3390/agronomy9110710

2. Shelton AM, Long SJ, Walker AS, Bolton M, Collins HL, Revuelta L, et al. First field release of a genetically engineered, self-limiting agricultural pest insect: evaluating its potential for future crop protection. *Front Bioeng Biotechnol.* (2020) 7:482. doi: 10.3389/fbioe.2019.00482

3. Chowdhury J, Al Basir F, Takeuchi Y, Ghosh M, Roy K. A mathematical model for pest management in Jatropha curcas with integrated pesticides-an optimal control approach. *Ecol Complex.* (2019) 37:24–31. doi: 10.1016/j.ecocom.2018.12.004

4. Pratiwi NP, Aldila D, Handari BD, Simorangkir GM. November. A mathematical model to control Mosaic disease of Jatropha curcas with insecticide and nutrition intervention. *AIP Conf Proc.* (2020) 2296:020096. doi: 10.1063/5.0030426

5. Liu S, Huang M, Wang J. Bifurcation control of a delayed fractional mosaic disease model for jatropha curcas with farming awareness. *Complexity.* (2020) 2020:2380451. doi: 10.1155/2020/2380451

6. Al Basir F, Ray S. Impact of farming awareness based roguing, insecticide spraying and optimal control on the dynamics of mosaic disease. *Ricerche Matematica.* (2020) 69:393–412. doi: 10.1007/s11587-020-00522-8

7. Wei X, Wang L, Jia Q, Xiao J, Zhu G. Assessing different interventions against Avian Influenza A (H7N9) infection by an epidemiological model. *One Health.* (2021) 13:100312. doi: 10.1016/j.onehlt.2021.100312

8. Ratchford, C. *Multi-scale and multi-group modeling techniques applied to Cholera and COVID-19 (Dissertation)*. The University of Tennessee at Chattanooga, Chattanooga, TN, United States. (2021).

9. Kwasi-Do Ohene Opoku N, Afriyie C. The role of control measures and the environment in the transmission dynamics of cholera. *Abstract Appl Anal.* (2020) 2020:2485979. doi: 10.1155/2020/2485979

10. Moore SE, Okyere E. Controlling the transmission dynamics of COVID-19. *arXiv[Preprint].arXiv:2004.00443*. (2020).

11. Van der Plank JE. Dynamics of epidemics of plant disease: Population bursts of fungi, bacteria, or viruses in field and forest make an interesting dynamical study. *Science.* (1965) 147:120–4. doi: 10.1126/science.147.3654.120

12. Noviello A, Romeo F, De Luca R. Time evolution of non-lethal infectious diseases: a semi-continuous approach. *Eur Phys J B Cond Matter Complex Syst.* (2006) 50:505–11. doi: 10.1140/epjb/e2006-00163-4

13. Stella IR, Srivastav AK, Ghosh M. May. Modeling and analysis of vector-borne plant disease with two delays. *J Phys Conf Series.* (2021) 1850:012125. doi: 10.1088/1742-6596/1850/1/012125

14. Al Basir F. A multi-delay model for pest control with awareness induced interventions—Hopf bifurcation and optimal control analysis. *Int J Biomath.* (2020) 13:2050047. doi: 10.1142/S1793524520500473

15. Ray S, Al Basir F. Impact of incubation delay in plant–vector interaction. *Math Comput Simul.* (2020) 170:16–31. doi: 10.1016/j.matcom.2019.09.001

16. Abraha T, Al Basir F, Obsu LL, Torres DF. Pest control using farming awareness: Impact of time delays and optimal use of biopesticides. *Chaos Solitons Fractals.* (2021) 146:110869. doi: 10.1016/j.chaos.2021.110869

17. Phan T, Pell B, Kendig AE, Borer ET, Kuang Y. Rich dynamics of a simple delay host-pathogen model of cell-to-cell infection for plant virus. *Discrete Continuous Dyn Syst B.* (2021) 26:515. doi: 10.3934/dcdsb.2020261

18. Blyuss KB, Al Basir F, Tsygankova VA, Biliavska LO, Iutynska GO, Kyrychko SN, et al. Control of mosaic disease using microbial biostimulants: insights from mathematical modelling. *Ricerche Matematica.* (2020) 69:437–55. doi: 10.1007/s11587-020-00508-6

19. Alemneh HT, Kassa AS, Godana AA. An optimal control model with cost effectiveness analysis of Maize streak virus disease in maize plant. *Infect Dis Modell.* (2021) 6:169–82. doi: 10.1016/j.idm.2020.12.001

20. Amelia R, Anggriani N, Istifadah N, Supriatna AK. Dynamic analysis of mathematical model of the spread of yellow virus in red chili plants through insect vectors with logistical functions. *AIP Conf Proc.* (2020) 2264:040006. doi: 10.1063/5.0023572

21. Kendig AE, Borer ET, Boak EN, Picard TC, Seabloom EW. Host nutrition mediates interactions between plant viruses, altering transmission and predicted disease spread. *Ecology.* (2020) 101:e03155. doi: 10.1002/ecy.3155

22. Shaw AK, Igoe M, Power AG, Bosque-Pérez NA, Peace A. Modeling approach influences dynamics of a vector-borne pathogen system. *Bull Math Biol.* (2019) 81:2011–28. doi: 10.1007/s11538-019-00595-z

23. Chen-Charpentier B, Jackson M. Optimal control of plant virus propagation. *Math Methods Appl Sci.* (2020) 43:8147–57. doi: 10.1002/mma.6244

24. Jittamai P, Chanlawong N, Atisattapong W, Anlamlert W, Buensanteai N. Reproduction number and sensitivity analysis of cassava mosaic disease spread for policy design. *Math Biosci Eng.* (2021) 18:5069–93. doi: 10.3934/mbe.2021258

25. Chen-Charpentier B. Delays in plant virus models and their stability. *Mathematics.* (2022) 10:603. doi: 10.3390/math10040603

26. Zaky MA. Existence, uniqueness and numerical analysis of solutions of tempered fractional boundary value problems. *Appl Num Math.* (2019) 145:429–57. doi: 10.1016/j.apnum.2019.05.008

27. Banu MS, Raju I, Mondal S. A comparative study on classical fourth order and butcher sixth order Runge-Kutta methods with initial and boundary value problems. *Int J Mat Math Sci.* (2021) 3:8–21. doi: 10.34104/ijmms.021.08021

28. Hossen M, Ahmed Z, Kabir R, Hossan Z. A comparative investigation on numerical solution of initial value problem by using modified Euler method and Runge Kutta method. *ISOR J Math.* (2019) 15:2278–5728. doi: 10.9790/5728-1504034045

29. Kafle J, Thakur BK, Acharya G. Formulative visualization of numerical methods for solving non-linear ordinary differential equations. *Nepal J Math Sci.* (2021) 2:79–88. doi: 10.3126/njmathsci.v2i2.40126

30. Koroche KA. Numerical solution of first order ordinary differential equation by using Runge-Kutta method. *Int J Syst Sci Appl Math.* (2021) 6:1–8. doi: 10.11648/j.ijssam.20210601.11

31. Olivares A, Staffetti E. Uncertainty quantification of a mathematical model of COVID-19 transmission dynamics with mass vaccination strategy. *Chaos Solitons Fractals.* (2021) 146:110895. doi: 10.1016/j.chaos.2021.110895

32. Campos C, Silva CJ, Torres DF. Numerical optimal control of HIV transmission in Octave/MATLAB. *Math Comput Applic.* (2019) 25:1. doi: 10.3390/mca25010001

33. Fatmawati MAK, Bonyah E, Hammouch Z, Shaiful EM. A mathematical model of tuberculosis (TB) transmission with children and adults groups: a fractional model. *Aims Math.* (2020) 5:2813–42. doi: 10.3934/math.2020181

34. Bürger R, Chowell G, Gavilán E, Mulet P, Villada LM. Numerical solution of a spatio-temporal predator-prey model with infected prey. *Math Biosci Eng.* (2019) 16:438–73. doi: 10.3934/mbe.2019021

35. Sweilam NH, Al-Mekhlafi SM, Assiri T, Atangana A. Optimal control for cancer treatment mathematical model using Atangana–Baleanu–Caputo fractional derivative. *Adv Diff Equat.* (2020) 2020:1–21. doi: 10.1186/s13662-020-02793-9

36. Curtiss CF, Hirschfelder JO. Integration of stiff equations. *Proc Natl Acad Sci.* (1952) 38:235–43. doi: 10.1073/pnas.38.3.235

37. Ebadi M, Gokhale MY. Hybrid BDF methods for the numerical solutions of ordinary differential equations. *Num Alg.* (2010) 55:1–17. doi: 10.1007/s11075-009-9354-4

38. Cash J. Efficient numerical methods for the solution of stiff initial-value problems and differential algebraic equations. *Proc R Soc Lond Ser A Math Phys Eng Sci.* (2003) 459:797–815. doi: 10.1098/rspa.2003.1130

39. Ogunrinde RB, Fadugba SE, Okunlola JT. On some numerical methods for solving initial value problems in ordinary differential equations. On Some Numerical Methods for Solving Initial Value Problems in Ordinary Differential Equations. (2012).

40. Lapidus L, Schiesser WE. *Numerical Methods for Differential Systems: Recent Developments in Algorithms, Software, and Applications.* (1976). doi: 10.1016/C2013-0-11041-0

41. Shampine LF. *Numerical Solution of Ordinary Differential Equations*. New York, NY: Routledge (2018). doi: 10.1201/9780203745328

42. Nasarudin AA, Ibrahim ZB, Rosali H. On the integration of stiff ODEs using block backward differentiation formulas of order six. *Symmetry.* (2020) 12:952. doi: 10.3390/sym12060952

43. Samson O, Victor JK. An application of second derivative ten step blended block linear multistep methods for the solutions of the holling tanner model and van der pol equations. *Covenant J Phys Life Sci.* (2019) 7:1–11. doi: 10.20370/s8gx-ft87

44. Qin G, Lou W, Wang H, Wu Z. *High Efficiency and Precision Approach to Milling Stability Prediction Based on Predictor-Corrector Linear Multi-Step Method.*

London: The International Journal of Advanced Manufacturing Technology (2022). doi: 10.21203/rs.3.rs-1456269/v1

45. Naz S, Raja MAZ, Mehmood A, Zameer A, Shoaib M. Neuro-intelligent networks for Bouc–Wen hysteresis model for piezostage actuator. *Eur Phys J Plus.* (2021) 136:1–20. doi: 10.1140/epjp/s13360-021-01382-3

46. Awan SE, Raja MAZ, Gul F, Khan ZA, Mehmood A, Shoaib M. Numerical computing paradigm for investigation of micropolar nanofluid flow between parallel plates system with impact of electrical MHD and Hall current. *Arabian J Sci Eng.* (2021) 46:645–62. doi: 10.1007/s13369-020-04736-8

47. Ghrist ML, Fornberg B, Reeger JA. Stability ordinates of Adams predictor-corrector methods. *BIT Num Math.* (2015) 55:733–50. doi: 10.1007/s10543-014-0528-7

48. Anwar N, Ahmad I, Raja MAZ, Naz S, Shoaib M, Kiani AK. Artificial intelligence knacks-based stochastic paradigm to study the dynamics of plant virus propagation model with impact of seasonality and delays. *Eur Phys J Plus.* (2022) 137:1–47. doi: 10.1140/epjp/s13360-021-02248-4

49. Shi R, Zhao H, Tang S. Global dynamic analysis of a vector-borne plant disease model. *Adv Diff Equat.* (2014) 2014:1–16. doi: 10.1186/1687-1847-2014-59

50. Jackson M, Chen-Charpentier BM. Modeling plant virus propagation with delays. *J Comput Appl Math.* (2017) 309:611–21. doi: 10.1016/j.cam.2016.04.024

51. Goel K. A mathematical and numerical study of a SIR epidemic model with time delay, nonlinear incidence and treatment rates. *Theory Biosci.* (2019) 138:203–13. doi: 10.1007/s12064-019-00275-5

52. Anggriani N, Amelia R, Istifadah N, Arumi D. October. Optimal control of plant disease model with roguing, replanting, curative, and preventive treatment. *J Phys Conf Series.* (2020) 1657:012050. doi: 10.1088/1742-6596/1657/1/012050

53. Janssen D, Ruiz L. Plant virus epidemiology. *Plants.* (2021) 10:1188. doi: 10.3390/plants10061188

54. Al Basir F, Takeuchi Y, Ray S. Dynamics of a delayed plant disease model with Beddington-DeAngelis disease transmission. *Math Biosci Eng.* (2021) 18:583–99. doi: 10.3934/mbe.2021032

55. Zhou X, Zhang L, Zheng T, Li HL, Teng Z. Global stability for a class of HIV virus-to-cell dynamical model with Beddington-DeAngelis functional response and distributed time delay. *Math Biosci Eng.* (2020) 17:4527–43. doi: 10.3934/mbe.2020250

56. Raja MAZ, Shah FH, Tariq M, Ahmad I. Design of artificial neural network models optimized with sequential quadratic programming to study the dynamics of nonlinear Troesch's problem arising in plasma physics. *Neural Comput Applic.* (2018) 29:83–109. doi: 10.1007/s00521-016-2530-2

57. Zahoor Raja MA, Shoaib M, El-Zahar ER, Hussain S, Li YM, Khan MI, et al. Heat transport in entropy-optimized flow of viscoelastic fluid due to Riga plate: analysis of artificial neural network. *Waves Random Complex Media.* (2022) 1–20. doi: 10.1080/17455030.2022.2028933

58. Ilyas H, Ahmad I, Raja MAZ, Shoaib M. A novel design of Gaussian WaveNets for rotational hybrid nanofluidic flow over a stretching sheet involving thermal radiation. *Int Commun Heat Mass Transfer.* (2021) 123:105196. doi: 10.1016/j.icheatmasstransfer.2021.105196

59. Soomro H, Zainuddin N, Daud H, Sunday J. Optimized hybrid block Adams method for solving first order ordinary differential equations. *Comput Mater Continua.* (2022) 72:2947–61. doi: 10.32604/cmc.2022.025933

60. Soomro H, Zainuddin N, Daud H, Sunday J, Jamaludin N, Abdullah A, et al. Variable step block hybrid method for stiff chemical kinetics problems. *Appl Sci.* (2022) 12:4484. doi: 10.3390/app12094484

61. Soomro H, Zainuddin N, Daud H. July. Convergence properties of 3-point block Adams method with one off-step point for ODEs. *J Phys Conf Series.* (2021) 1988:012038. doi: 10.1088/1742-6596/1988/1/012038

62. Abdi A, Hojjati G. Second derivative backward differentiation formulae for ODEs based on barycentric rational interpolants. *Num Alg.* (2021) 87:1577–91. doi: 10.1007/s11075-020-01020-6

63. Zhao J, Jiang X, Xu Y. A kind of generalized backward differentiation formulae for solving fractional differential equations. *Appl Math Comput.* (2022) 419:126872. doi: 10.1016/j.amc.2021.126872

64. Meyer T, Li P, Schweizer B. Backward differentiation formula and Newmark-type index-2 and index-1 integration schemes for constrained mechanical systems. *J Comput Nonlinear Dyn.* (2020) 15:021006. doi: 10.1115/1.4045505

65. Hu J, Shu R. On the uniform accuracy of implicit-explicit backward differentiation formulas (IMEX-BDF) for stiff hyperbolic relaxation systems and kinetic equations. *Math Comput.* (2021) 90:641–70. doi: 10.1090/mcom/3602

66. Wang R, Ding M, Wang Y, Xu W, Yan L. Field characterization of landslide-induced surge waves based on computational fluid dynamics. *Front Phys.* (2022) 9:813827. doi: 10.3389/fphy.2021.813827

67. Brenneisen J, Daub A, Gerach T, Kovacheva E, Huetter L, Frohnapfel B, et al. Sequential coupling shows minor effects of fluid dynamics on myocardial deformation in a realistic whole-heart model. *Front Cardiovasc Med.* (2021) 8:768548. doi: 10.3389/fcvm.2021.768548

68. Awan SE, Awais M, Raja MAZ, Parveen N, Ali HM, Khan WU, et al. Numerical treatment for dynamics of second law analysis and magnetic induction effects on ciliary induced peristaltic transport of hybrid nanomaterial. *Front Phys.* (2021) 9:631903. doi: 10.3389/fphy.2021.631903

69. Ferdian E, Suinesiaputra A, Dubowitz DJ, Zhao D, Wang A, Cowan B, et al. 4DFlowNet: super-resolution 4D flow MRI using deep learning and computational fluid dynamics. *Front Phys.* (2020) 8:138. doi: 10.3389/fphy.2020.00138

10.3389/fams.2022.1001392

Nomenclature

Symbols			
N	Total plant density	r	Plants' natural fatality rate
c	Plants' increased fatality rate	m	Plants' proliferation rate
$S(t)$	Susceptible plants	$X(t)$	Susceptible vectors
$I(t)$	Infected plants	$Y(t)$	Infectious plants
$S(t_0)$	Initial conditions for $S(t)$	$X(t_0)$	Initial conditions for $X(t)$
$I(t_0)$	Initial conditions for $I(t)$	$Y(t_0)$	Initial conditions for $Y(t)$
Greek Letters			
γ	Infection ratio of a susceptible plant by an infected vector,	γ_1	Infection ratio of vectors by infected plants
υ	Plants' natural fatality rate	Ω	Vector replenishment rate
δ	Time delay		
Abbreviations			
ODEs	Ordinary differential equations	ADM	Adams method
COVID-19	Coronavirus disease of 2019	BDF	Backward differentiation formula
HIV	Human immunodeficiency virus	PVPMV	Plant virus propagation by a vector
DDEs	Delay differential equations		